Plant Physiology and Biochemistry 143 (2019) 94–108

Contents lists available at ScienceDirect

Plant Physiology and Biochemistry

journal homepage: www.elsevier.com/locate/plaphy

Research article

Effects of simulated atmospheric nitrogen deposition on foliar chemistry and physiology of hybrid poplar seedlings

Yanbo Hu[a,c,*], Andreas D. Peuke[b], Xiyang Zhao[c], Junxin Yan[d], Chunming Li[e]

[a] Key Laboratory of Saline-alkali Vegetation Ecology Restoration, Ministry of Education, College of Life Sciences, Northeast Forestry University, Harbin City, 150040, PR China
[b] ADP International Plant Science Consulting, Talstrasse 8, D-79194, Gundelfingen, Germany
[c] State Key Laboratory of Tree Genetics and Breeding, Northeast Forestry University, Harbin City, 150040, PR China
[d] College of Landscape Architecture, Northeast Forestry University, Harbin City, 150040, PR China
[e] Heilongjiang Academy of Forestry, Harbin City, 150081, PR China

ARTICLE INFO

Keywords:
Atmospheric nitrogen deposition
Crystal
Dark respiration
Free amino acid
Poplar
Polyamine

ABSTRACT

During recent decades, the southern and eastern regions of Asia have experienced high levels of atmospheric N deposition. Excess N deposition is predicted to influence tree growth and species composition in the regions, but visual or physiological assessments alone are not sufficient to determine the real effects of atmospheric N deposition. In this study, we simulated atmospheric wet deposition of inorganic N by spraying a NO_3^- solution (20 mmol·L^{-1}) or a mixture of NO_3^- (20 mmol·L^{-1}) plus NO_2^- (100 or 300 μmol·L^{-1}) on leaves of hybrid poplar (*Populus alba* × *Populus berolinensis*) seedlings and examined morphoanatomical traits and physiological processes. Leaves of seedlings sprayed with single or mixed N solutions developed marginal necrosis, curling, and small cracks on the adaxial surface. The silicon (Si)-rich crystals were larger (about 100% increase in crystal diameter compared to untreated seedlings) on the adaxial leaf surface, with a significant positive correlation between the atomic percentage of N and Si on the crystal areas of the surface. Leaves were sensitive to NO_2^- compared with NO_3^- even at a low concentration; water content, dry mass, and photochemical variables significantly declined and dark respiration increased only in leaves treated with mixed N form. Mixed N foliar applications significantly increased leaf concentrations of the free amino acids Glu, Gln, and Asn and organic acids oxaloacetic acid and citric acid. Besides, mixed N treatment stimulated leaf transamination, as indicated by significant increases in Ala and Asp concentrations and activities of glutamic oxalacetic transaminase and glutamic pyruvic transaminase. However, mixed N applications led to declines in leaf concentrations of putrescine (by 65%, $p = 0.01$) and spermine (by 53%, $p = 0.01$). A higher proportion of NO_2^- (300 μmol·L^{-1}) in mixed N solution was inhibitory to key N-metabolic enzymes and N translocation via the phloem. Our results showed that wet deposition of airborne N pollutants modified surface properties and induced additional detrimental effects related to N-compound foliar absorption. Furthermore, our findings indicate that detoxification of reactive N is apparently related to N assimilation and export from the treated leaves via the phloem.

1. Introduction

During the past two decades (1995–2015), atmospheric reactive N species and their deposition have increased continuously at a global scale (Stevens et al., 2018). In some regions of Asia, atmospheric inorganic N is mainly wet-deposited in mixed N forms (Liu et al., 2011). A dominant deposition N form in the regions of Japan and China was NO_3^--N, and NO_2^--N accounted for a small fraction of total N deposition (Hayashi et al., 2007; Chen et al., 2019). In previous simulations of inorganic N wet deposition, NO_3^- or NH_4NO_3 solutions of different concentrations have been often used (Liao et al., 2010; Mao et al., 2018); however, less emphasis has been placed on NO_2^- or a mixture of NO_3^- and NO_2^-. A mixed N species may be more realistic for simulating atmospheric inorganic N deposition.

Atmospheric N deposition can influence plant growth either via leaves or roots (Bourgeois et al., 2019). Root-originating impacts are indirectly through N deposition-mediated soil acidification and changes in soil microbial diversity (Liu et al., 2011). Foliar N deposition directly

* Corresponding author. Key Laboratory of Saline-alkali Vegetation Ecology Restoration, Ministry of Education, College of Life Sciences, Northeast Forestry University, Harbin City, 150040, PR China.
E-mail address: huybnefu@yahoo.com (Y. Hu).

https://doi.org/10.1016/j.plaphy.2019.08.023
Received 23 April 2019; Received in revised form 27 August 2019; Accepted 27 August 2019
Available online 30 August 2019
0981-9428/

Abbreviations

CA	citric acid
CAA	*cis*-aconitic acid
CXP	collision cell exit potential
DW	dry weight
E	transpiration rate
EDX	energy dispersive X-ray analysis
EP	entrance potential
EtN	cholamine
FA	fumaric acid
GAGA	γ-aminobutyric acid
GOT	glutamic-oxalacetic transaminase
GPT	glutamic-pyruvic transaminase
IS	ionspray voltage
KA	α-ketoglutaric acid
Lys	lysine
MA	malic acid
NR	nitrate reductase
NiR	nitrite reductase
OAA	oxaloacetic acid
PA	pyruvic acid
Phe	phenylalanine
Pn	net photosynthetic rate
Put	putrescine
R_{dark}	dark respiration rate
SA	succinic acid
Ser	serine
Si	silicon
Spd	spermidine
Spm	spermine
SS	soluble sugars
TEM	ion source temperature
TCA	tricarboxylic acid cycle
TRo/RC	trapping flux leading to QA reduction per RC
Trp	tryptophan
WUE	water-use efficiency

affects plant growth after N absorption through stomata or the cuticle and subsequent N assimilation via the GS-GOGAT cycle pathway into amino acids (AAs) (Masclaux-Daubresse et al., 2010). Key N metabolic enzymes are inducible by N addition (Su et al., 2019), their changes have significant impacts on plant N status (Liu et al. 2016, 2018).

Morphological and anatomical traits are commonly evaluated in simulations to determine the real effects of atmospheric acid deposition (Sant'Anna-Santos et al., 2006). The incidence and severity of visible leaf injury is considered a good indicator of the sensitivity or tolerance of a plant species to atmospheric N deposition, although many variables such as plant species, age of tissue and plants, foliar surface characters, and environmental factors can also influence the extent of injury (Bitterlich and Upadhyaya, 1990). Some plant species (such as *Senecio vulgaris* and cole crops) with potentially lower amounts of epicuticular waxes or more permeable cuticles are more susceptible to foliar N application and solute injury (Bitterlich and Upadhyaya, 1990). Spraying conditions (e.g., solution concentration, application dose or environmental conditions) of the simulated acid solutions may also influence the outcome (Fernández et al., 2017).

N deposition can also cause the imbalance between C and N metabolism, resulting in a significant increase in major organic N components (free AAs such as Glu, Gln, Asn, and Arg) and a decline in C assimilation (Mao et al., 2018). These amino acids are considered cellular sensors of N status (Mattoo et al., 2010), and their biosynthesis in plant leaves are very sensitive to atmospheric N deposition (Xu and Xiao, 2017). Polyamines (putrescine, spermidine, and spermine), which interact with the metabolism of AAs (Mattoo et al., 2010) and photosynthesis, can be another bio-indicators of plant sensitivity to N deposition (Minocha et al., 2000). Moreover, leaf respiration rates show a dose-dependent correlation with reactive N (Singh and Singh, 1978). Exogenous inorganic N such as NO_3^- enters a leaf mainly through stomata, with a small fraction diffusing through the cuticle (Sutton et al., 1995; Peuke et al., 1998a). So excess N deposition influences leaf surface characters, leading to stomatal dysfunction (Liao et al., 2010) and changes in surface chemistry (Hu et al., 2014) and surface wetting (Peuke et al., 1998b). Besides, foliar applications of NO_3^- or NH_4^+ may affect uptake and transport of cations such as K^+, Na^+, Mg^{2+}, Ca^{2+}, anions such as Cl^-, NO_3^-, $H_2PO_4^-$, and signal compounds (ABA) in the plant tissues (Peuke et al., 1998a, b). Foliar NH_4^+ sprays lead to a smaller cross-sectional area of hyaline leaf cells and hyaline to chlorophyllose cell area ratio compared to the controls, whereas NO_3^- applications had the opposite effect (Manninen et al., 2011).

Besides the type of N inputs (form, timing, or amount), plant species is another important factor determining plant performance after N deposition (Bourgeois et al., 2019). In general, plant species with fast growth and high N-use efficiency do better when inorganic N deposition is high (Payne et al., 2013). The genus *Populus*, including one of the fastest growing trees and is widely distributed over the northern hemisphere (Rennenberg et al., 2010), commonly have a high N uptake rate and use efficiency, particularly for NO_3^- (Rennenberg et al., 2010). Therefore, poplar trees such as *Populus tremuloides* can grow well after applications of low concentrations of foliar NO_3^- (Karnosky et al., 1992). In the urban areas, poplar species have a higher NO_2 assimilation rate than other roadside trees (Takahashi et al., 2005), but excess N deposition inevitably inhibits growth (Karnosky et al., 1992), partially due to foliar injury and physiological disorders (Elvir et al., 2006; Hu and Sun, 2010). The extent and type of the foliar injury caused by inorganic N species are associated with the concentration and the nature of N species (Kannan and Charnel, 1986).

Despite many studies simulating inorganic N wet deposition, most of the studies focused on the effects of a single N form on plant growth. However, the effects of mixed N forms (particularly NO_3^- plus NO_2^-) on tree growth are unavailable. Moreover, visual or physiological assessments alone are indicative of plant responses to N addition, but are not sufficient to determine the actual effects of atmospheric N deposition. In this study, carried out with a hybrid poplar (*Populus alba* × *P. berolinensis*) commonly planted in northern China, two independent experiments were conducted to simulate daily inorganic N wet deposition by spraying the foliage with a single NO_3^- solution or different ratios of a mixed NO_3^-/NO_2^- solution. We hypothesized that (1) inorganic N depositions altered leaf morphoanatomical traits and physiological processes, and that (2) foliar-applied mixed N species and single N form caused different plant responses. Assessments were mainly focused on visible leaf injury, surface chemical traits, and key C and N metabolism in response to inorganic N application.

2. Materials and methods

2.1. Plant material

The hybrid poplar, *Populus alba* × *P. berolinensis*, a main urban greening tree species in northern China, was propagated from 2-year-old cuttings, which were collected from Heilongjiang Academy of Forestry. The cuttings were cultivated in 2.6-L pots filled with an 8:1:1 (v:v:v) black soil–vermiculite–sand mixture (P: 0.40 g·kg^{-1}, N: 0.93 g·kg^{-1}, organic matter: 23.97 g·kg^{-1}) and grown outside; in case of rain, the cuttings were brought to a covered place adjacent to the original position. This rainproof measure can ensure the cuttings not to

be influenced by the rainfall factor. The cuttings were watered with tap water every 2 days. Physical and chemical properties of tap water were obtained from the Water Quality Report (Harbin Water Supply Group Co., Ltd, 2018).

2.2. Experimental design

Two independent experiments were set up to assess (1) morphological and physiological responses of poplar leaves to foliar sprays of a NO_3^- solution and a NO_3^-/NO_2^- mixed solution and (2) responses of C and N metabolites to sprays of a NO_3^-/NO_2^--mixed solution with different ratios.

Experiment 1 (Exp. 1): When the seedlings were about 90 cm tall, 60 seedlings were divided into three treatment groups (20 plants per group): Group 1, control treatment (tap water, 0.08 mmol·L^{-1} $NaNO_3^-$, pH 6.9); Group 2, NO treatment (20 mmol·L^{-1} $NaNO_3$ solution, pH 5.17), Group 3, NNO treatment (mixed solution of 20 mmol·L^{-1} $NaNO_3$ and 100 μmol·L^{-1} $NaNO_2$, pH 5.09). Spray N concentrations were selected based on the trials by Sun et al. (2015), Chen et al. (2019), and our previous experiments (Wang et al. 2015, 2017). In the literature (Sun et al., 2015; Chen et al., 2019), the monthly mean NO_3^--N concentrations in precipitation ranged approximately from 10 to 50 mmol L^{-1} in the growing seasons. In our previous studies (Wang et al. 2015, 2017), different inorganic N concentrations (10–50 mmol·L^{-1}) were used for leaf spraying, and 20 mmol·L^{-1} was found to be suitable for studies on plant physiological response. Upper and lower leaf surfaces were sprayed daily (except in the case of rain) with 40 mL of the solution per plant for 21 days. The amount (40 mL·$plant^{-1}$) was the mean volume of solution which remained on the plants of this size after spraying. The spray amount and frequency were based on our previous experiments (Wang et al. 2015, 2017), with simultaneous consideration of poplar physiological responses and root growth under pot experimental conditions. Three (2 continuous plus another one) rainy days occurred during the treatment period; no spray treatment in a rainy day was based on the consideration that spraying treatment during the temporary rainproof treatment could produce unexpected impacts on the young leaves due to possibly extended stay time of the solutes (under the changed environmental conditions such as wind speed and temperature). According to the previous studies (e.g., Bitterlich and Upadhyaya, 1990; Fernández et al., 2017), the stay time of sprayed solutes on a leaf is a factor affecting leaf morphophysiological response. A longer treatment period was not suitable for a pot experiment because root growth would be influenced by a limited pot volume. During the study, environmental conditions were monitored from 9:00 to 12:00 a.m. and corresponded to mean ambient temperature of 29.6 °C (max/min temp of 32.1 °C/25.5 °C), 45% relative humidity (RH), 380 μL·L^{-1} atmospheric CO_2 concentration, and 400–1600 μmol·m^{-2}·s^{-1} photosynthetic photon flux density (PPFD). Photosynthetic variables, dark respiration rate, and water-use efficiency were nondestructively measured on treatment days 7, 14, and 21. Leaf surface features, metabolite concentrations, and biomass were measured on day 21.

Experiment 2 (Exp. 2): When the plants were about 110 cm tall, 18 seedlings were transferred to a plant culture chamber (at 24 ± 2 °C, 55% RH, 16 light/8 h dark, 200 μmol·m^{-2}·s^{-1} PPFD provided by fluorescent tubes, and about 480 μL·L^{-1} CO_2), and watered with a modified Hoagland's nutrient solution every 3 days. After adaptive growth for 2 weeks, seedlings developed three or four new leaves and were divided into three treatment groups (six plants per group): Group 1: control treatment (tap water, 0.08 mmol·L^{-1} $NaNO_3^-$, pH 6.5); Group 2: NNO100 treatment (mixed solution of 20 mmol·L^{-1} $NaNO_3$ and 100 μmol·L^{-1} $NaNO_2$, pH 5.01), and Group 3: NNO300 treatment (mixed solution of 20 mmol·L^{-1} $NaNO_3$ and 300 μmol·L^{-1} $NaNO_2$, pH 5.16). Plants were sprayed as described for Exp. 1 but only 14 days. Key enzyme activities and metabolite concentrations were measured on day 14.

2.3. Measurements

2.3.1. Leaf epidermal characters

Leaf samples were washed with distilled water and then cut into 2 × 3 mm fragments. Transversal sections and adaxial and abaxial surfaces were mounted on SEM stubs and sputtered with 10 nm gold-palladium (BAL-TEC, SCD 005, Germany). Stomata, cuticle/epidermis, and palisade/spongy tissue were then viewed by scanning electron microscopy (SEM, FEI Quanta 200, FEI Inc., USA), and surface-chemical properties (element composition and atomic percent) were analyzed by energy dispersive X-ray spectrometer (EDX, Oxford Instruments, Oxfordshire, UK). Leaf surfaces were imaged at magnifications between 100 and 2000, with 15 kV acceleration voltage, 10 mm working distance, 2.26 A filament current and 99 μA emission current.

2.3.2. Leaf dry mass and absolute water content

Fresh weight (FW, 57 fully expanded leaves collected from six plants) was measured; dry weight (DW) was measured after oven-drying at 80 °C to a constant mass. Absolute water content (AWC) of leaves was calculated as described by Ghashghaie et al. (1992): AWC = (FW − DW)/DW.

2.3.3. Gas exchange variables, leaf temperature, and water-use efficiency

In Exp. 1, gas exchange variables were measured for the third fully expanded leaf (from the top) using a LI-6400 photosynthesis system (LI-COR, Lincoln, Nebraska, USA). Net CO_2 assimilation rate (Pn), transpiration rate (E) and stomatal conductance (Gs) were determined at 380 μL·L^{-1} CO_2, 65% RH, and 1000 μmol·m^{-2}·s^{-1} PPFD. Then dark respiration rate (R_{dark}), air temperature, and leaf temperature were measured at a PPFD from 1000 μmol m^{-2}·s^{-1} to 0 μmol m^{-2}·s^{-1} (LED light source provided by an automatic control device of the LI-6400) with the leaf chamber covered by an opaque sheet to block natural light. Measurements were performed on sunny mornings between 9:00 a.m. and 11:00 a.m. Water-use efficiency (WUE) was calculated as WUE = Pn·E^{-1}.

2.3.4. Chlorophyll fluorescence variables

Photochemical and nonphotochemical quenching variables for leaves were measured using a portable fluorometer (Handy PEA, Hansatech Instruments Ltd., Norfolk, UK). Leaves were first dark-adapted for 30 min, then exposed to a saturating red light pulse (650 nm, 3000 μmol photons·m^{-2}·s^{-1}) provided by an array of six light-emitting diodes. Chlorophyll fluorescence variables were calculated automatically in Handy PEA v 1.3 software: ABS/RC: absorption flux per PSII reaction center (RC), DIo/RC: dissipated energy flux per RC at t = 0, ETo/RC: electron transport flux per RC at t = 0, ETo/TRo: probability that a trapped exciton moves an electron into the electron transport chain beyond QA at t = 0, Fv/Fo: ratios characterizing the efficiency of PSII, TRo/RC: trapping flux leading to QA reduction per RC.

2.3.5. Nitrate reductase activity and NO_3^- concentration

The fourth to fifth fully expanded leaves from the top of the plants were collected, washed with distilled water, and cut into fragments (about 0.3 × 0.4 cm), of about 0.5 g each, for the nitrate reductase (NR) assay. NR activity was assayed in vivo using the method of Streeter and Bosler (1972) but using vacuum infiltration.

For measuring leaf NO_3^- concentration, 0.5 g of ground samples were dissolved in 50 mL deionized water in a volumetric flask. After the solution was mixed well, soaked for 24 h, and filtered through a 0.45 μm syringe filter, the filtrate was diluted 2-fold with deionized water. Then leaf NO_3^- concentration in 1 mL of the filtrate was analyzed using ion chromatography and a METROSEP A SUPP 5–150 column (4 mm × 150 mm, 5 μm) (Metrohm Ltd, Herisau, Switzerland) according to the procedure of Shah et al. (2013) with minor revisions: a mixed eluent solution of 3.2 mM Na_2CO_3 and 1.0 mM $NaHCO_3$,

injection volume of 1 μL, flow rate of 0.70 mL·min^{-1}, column temperature of 30 °C. The diode array detector (DAD) was set to 210 nm. The concentration of NO_3^- was determined using linear regression equations of the standard curves.

2.3.6. Free amino acid composition and free polyamine concentration

One gram of the leaf samples were ground to a fine powder in liquid N and then hydrolyzed in 3.5 mL deionized water. Samples were diluted and derivatized as done by Gao et al. (2017). The combined supernatant was labeled with iTRAQ reagents (API 50AA kit) as recommended by the manufacturer (Beijing Mass Spectrometry Medical Research Co., Ltd, Beijing) and then quantified by HPLC–MS/MS (UltiMate 3000 [Thermo Fisher Scientific Inc., Waltham, MA, USA]–API 3200 QTRAP [AB Sciex, Boston MA, USA]) using MSLAB HP-C18 column (150 mm long, 4.6 mm diameter, 5 μm particle size; Beijing Amino Acid Medical Research Co.), flow rate of 0.8 mL·min^{-1}, column temperature of 50 °C; solvent A (water with 0.1% methanoic acid) and solvent B (acetonitrile with 0.1% methanoic acid). Mass spectrometry (MS) conditions were set as described by Jin et al. (2016) with minor modifications (IS: +5500 V; TEM: 500 °C; EP: +10; and CXP: +2.0).

Additionally, 1 g leaves were ground to a fine powder in liquid N and then extracted in 3.7 mL 5% (w/v) perchloric acid. Samples were centrifuged at 15000 *g* at 4 °C for 30 min, and the supernatant was kept for further analysis. Following dansylation (Song et al., 2001), free polyamines (Put, Spd, and Spm) in the supernatant were determined by HPLC-MS/MS (Ultimate3000-API 3200 Q TRAP) using MSLAB HP-C18 column (150 mm long, 4.6 mm diameter, 5 μm particle size). Two solvents, solvent A (water) and solvent B (acetonitrile), were delivered to the column at a flow rate of 1 mL·min^{-1}. Elution was operated as described by Gao et al. (2017).

2.3.7. Chlorophyll index, total free amino acids, and soluble sugars

Chlorophyll index (SPAD value) of the midpoint of the third and fourth fully-expanded leaves (from the top) was measured by A SPAD meter (SPAD-502, Minolta Camera Co., Osaka, Japan). Fresh samples (100 mg leaf, petiole, or stem bark) were ground to a fine powder in liquid N and then hydrolyzed in 1 mL deionized water. The homogenates were transferred to a 1.5-mL centrifuge tube and boiled at 95 °C for 15 min, then cooled with tap water. The tubes were then centrifuged at 8000 *g* at 4 °C (total free AAs) or 25 °C (soluble sugars) for 10 min. The metabolite concentration was estimated separately using free AAs and soluble sugar assay Kits (Comin Biotechnology Co. Ltd, Suzhou, China) and the manufacturer's instructions.

2.3.8. Total free fatty acids and total sugars

Fresh leaves were ground to a fine powder in liquid N, then 100 mg samples were weighed and hydrolyzed in 1 mL deionized water and vortexed. After 3 h, the homogenates were centrifuged at 8000 *g* at 4 °C for 10 min, then 0.4 mL of the supernatant was used for the chromogenic reaction of free fatty acids (FAs) with copper acetate, and 200 μL was used to estimate the concentration of total free FAs by measuring absorbance at 715 nm. Additionally, 100 mg of samples were hydrolyzed, boiled, diluted, centrifuged, and used in the chromogenic reaction of reducing sugar with 3,5-dinitrosulfosalicylic acid, then absorbance was measured at 540 nm. The concentration of free FAs and total sugars was determined separately using linear regression equation of the standard curve.

2.3.9. Nitrite reductase, glutamic pyruvic transaminase, glutamic oxalacetic transaminase

The activity of the key N metabolic enzymes was assayed separately

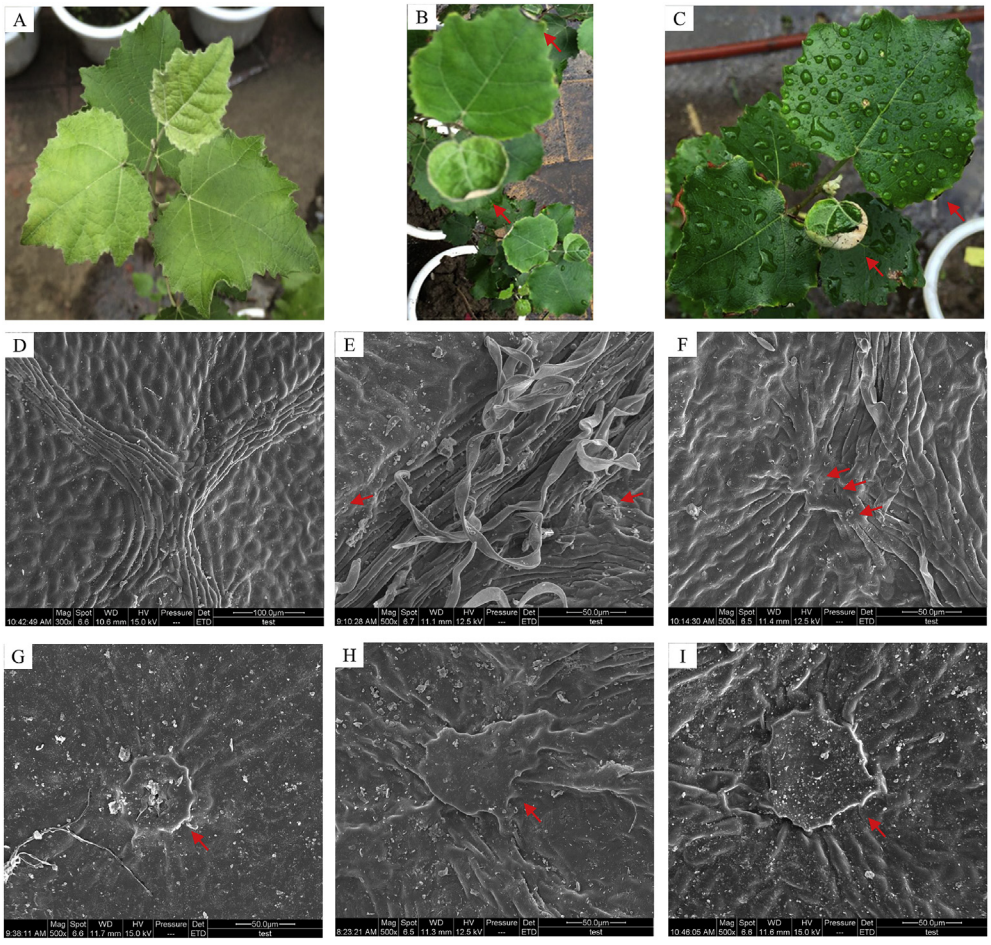

Fig. 1. Morphological and epicuticular traits of leaves from 2-year-old poplar seedlings (*Populus alba* × *P. berolinensis*) after 21 days of foliar spraying with tap water (control; A, D, G), NO_3^- solution (NO: 20 mmol·L^{-1}; B, E, H) or NO_3^- plus NO_2^- solution (NNO: 20 mmol·L^{-1} NO_3^- plus 100 μmol·L^{-1} NO_2^-; C, F, I). Scanning electron micrographs of the adaxial leaf surface (D–I). Red arrows indicate visible leaf injury (Fig. 1B and C), small cracks and tissue collapse (Fig. 1E and F), and crystals (Fig. 1 G–I). Note: Average crystal diameter was 41.54 ± 11.63 μm for the control leaves (n = 9), 86.09 ± 35.65 μm for NO-treated leaves (n = 7), and 80.23 ± 33.77 μm for NNO-treated leaves (n = 9), with statistically significant differences between means of the control and N-sprayed leaves (p < 0.05 by Tukey's HSD test), no significant difference between means of NO and NNO treatment (p = 0.74). (For interpretation of the references to colour in this figure legend, the reader is referred to the Web version of this article.)

using nitrite reductase, glutamic pyruvic transaminase, glutamic oxalacetic transaminase assay kits (Comin Biotechnology Co. Ltd, Suzhou, China) in a 96-well culture plate. Fresh leaf samples (100 mg) were ground in liquid N and homogenized in 1 mL extraction buffer (PBS, pH 7.4), then centrifuged at 8000 *g* at 4 °C for 10 min. The supernatants were collected, diluted and incubated at 37 °C for 30 min or 25 °C for 60 min according to the manufacturer's instructions. Enzyme activity was calculated based on the absorbance values and a standard curve.

2.3.10. Organic acids in the tricarboxylic acid cycle

Leaf samples (1 g) were ground in liquid N and hydrolyzed in 3.5 mL deionized water. Then 50 µL of the solution was added to 200 µL of methanol (containing the internal standards). After samples stood for 1 min, they were centrifuged at 13,000 *g* at 4 °C for 4 min. The supernatant was collected and analyzed by HPLC-MS/MS (UltiMate 3000–API 3200 Q TRAP) in negative ion mode using MSLab HP-C18 column (150 mm long, 4.6 mm diameter, 5 µm particle size; flow rate of 1 mL·min^{-1}; column temperature of 50 °C). Solvent A (water with 2 mmol·L^{-1} ammonium formate) and solvent B (acetonitrile with 2 mmol·L^{-1} ammonium formate) were used as mobile phases for elution as described by Gao et al. (2017). Mass spectrometry conditions were done as described by Jin et al. (2016).

2.4. Statistical analyses

Before the analysis of variance and testing for statistical significance, the normality of data distribution and homogeneity of variance were checked using the Kolmogorov–Smirnov test and Levene's test, respectively. Logarithmic transformations were used if the data did not meet the assumptions of normality and homogeneity of variance. For Exp. 1, data in the forms of macroscopic and microscopic pictures were analyzed descriptively and comparatively. Chemical elements on the leaf surface and the physiological indexes (mean ± SD, $n = 6$) were assessed by a one-way ANOVA, followed by Tukey's HSD test to analyze any difference between the control and treatments. Differences were considered significant at $p < 0.05$. Correlation of the atomic percentage of the chemical elements was analyzed by using Pearson correlation coefficient (r) and linear regression analysis; statistical significance of the model and the regression coefficient was verified by an F-test and Student's t-test, respectively, at $p < 0.05$. Mean metabolite concentration and enzyme activity in Exp. 2 ($n = 4$) were analyzed using a one-way ANOVA, followed by Tukey's HSD test ($p < 0.05$). The analyses were performed using Excel software (Microsoft, Redmond, WA, USA), and IBM SPSS Statistics 20.0 (StataCorp, College Station, TX, USA).

3. Results

3.1. Leaf morphoanatomical traits

Foliar applications of NO and NNO resulted in marginal necrosis and inward curling of both immature and mature leaves (red arrows in Fig. 1B and C). Small cracks (red arrows in Fig. 1E and F) occurred on the epicuticular wax layer of the N-treated leaves. Additionally, crystals (red arrows) were observed on untreated (Fig. 1G), NO-, and NNO-treated leaves (Fig. 1H and I); the diameters of these epicuticular crystals were larger on the N-treated leaves than on untreated leaves. According to EDX-SEM examinations, crystals were rich in Si (Fig. A1).

Eight main chemical elements were quantified on the adaxial surface of control and treated leaves; C, N, O were the most abundant. Foliar applications of NO or NNO had no impacts on the atomic percentage of the quantified elements on non-crystal surfaces of leaves, but on crystal surfaces, NNO treatment led to increases in the atomic percentage of N ($p = 0.11$), O ($p < 0.01$), Mg ($p = 0.04$), Si ($p = 0.14$) and a decrease in C ($p < 0.01$) (Table A1). A correlation of atomic percentage (At %) between N and Si was not significant on the non-crystal surface of the control or NNO-treated leaves, whereas significant positive ($r = 0.55$, $p = 0.03$) on the crystal surface of NNO-treated leaves (Fig. A2).

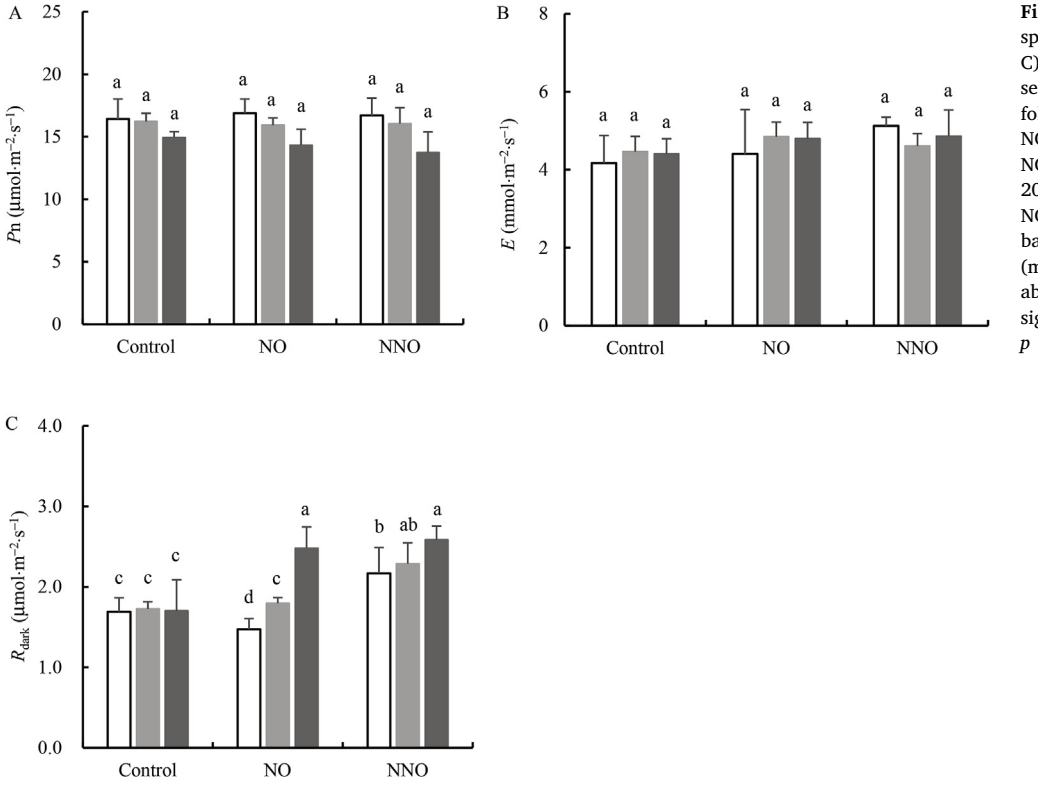

Fig. 2. Net photosynthetic (*Pn*, A), transpiration (*E*, B), and dark respiration (R_{dark}, C) rates of leaves from 2-year-old poplar seedlings (*P. alba* × *P. berolinensis*) after foliar spraying with tap water (control), NO_3^- solution (NO: 20 mmol·L^{-1}), and NO_3^- plus NO_2^- solution (NNO: 20 mmol·L^{-1} NO_3^- plus 100 µmol·L^{-1} NO_2^-) for 7 (white bars), 14 (light gray bars), and 21 (dark gray bars) days (means ± SD, $n = 6$). Different letters above the columns indicate statistically significant differences among means at $p < 0.05$ by Tukey's HSD test.

3.2. Leaf biomass, surface temperature, and water status

Compared to the control, NO treatment did not have any significant impact on leaf DW and WUE, whereas NNO treatment led to significant declines in DW (by 10%, $p < 0.05$) and WUE (by 13%, $p < 0.05$) (Fig. A3A, D). NO- and NNO-treated leaves had higher T_{leaf} and lower AWC than the control leaves ($p < 0.05$; Fig. A3B, C).

3.3. Photosynthetic performances and dark respiration rate

NO or NNO treatment had no significant impacts on *P*n and *E* during the 21 days (Fig. 2A and B), but R_{dark} significantly increased (Fig. 2C) and was higher in NNO-treated leaves than in the control and NO-treated leaves on day 7 and 14 ($p < 0.05$). Leaf photochemical processes were more sensitive to foliar applications of NO and NNO. ABS/RC and TRo/RC significantly decreased and ETo/TRo increased in leaves treated with NNO for 14 days. Compared to the control, NO and NNO treatments for 21 days caused significant decreases in ABS/RC, TRo/RC, ETo/RC and DIo/RC and increases in ETo/TRo and Fv/Fo (Table 1).

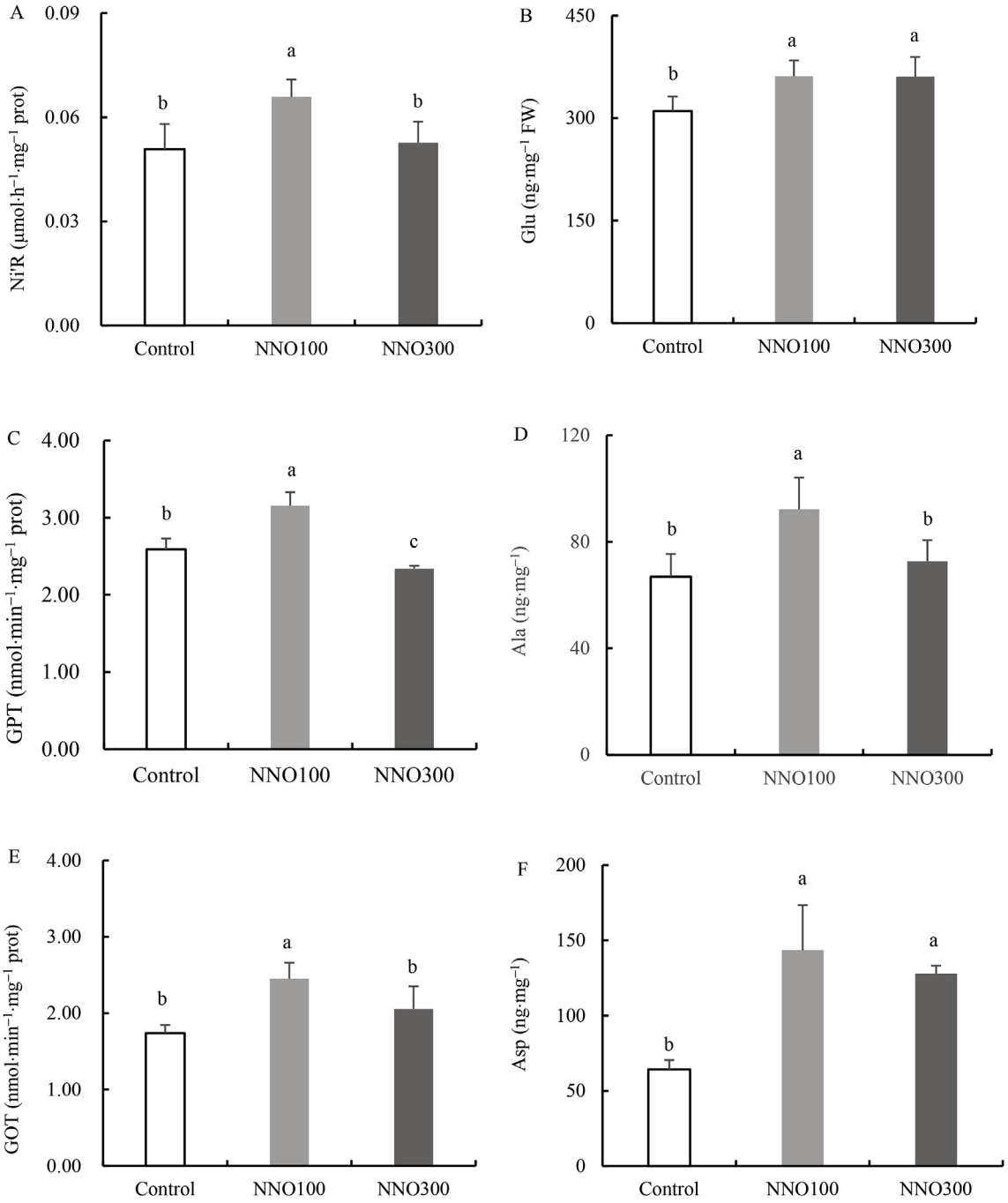

Fig. 3. Key enzyme activity (A, C, E) and metabolite concentration (B, D, F) of leaves from 2-year-old poplar seedlings (*P. alba* × *P. berolinensis*) after 14 days of foliar spraying with tap water (Control), and NO_3^- plus NO_2^- solutions (NNO100: 20 mmol·L^{-1} NO_3^- plus 100 μmol·L^{-1} NO_2^-, NNO300: 20 mmol·L^{-1} NO_3^- plus 300 μmol·L^{-1} NO_2^-) (means ± SD, $n = 4$). Different letters above the columns indicate statistically significant differences among means at $p < 0.05$ by Tukey's HSD test.

Table 1
Photochemical variables for fully-expanded leaves of 2-year-old poplar seedlings (*Populus alba* × *P. berolinensis*) after 14 and 21 days of foliar spraying (mean ± SD, $n = 6$).

Days	Treatment	ABS/RC	TRo/RC	ETo/RC	ETo/TRo	DIo/RC	Fv/Fo
14	Control	1.31 ± 0.05 a	1.07 ± 0.04 a	0.70 ± 0.04 a	0.65 ± 0.03 b	0.23 ± 0.02 a	4.67 ± 0.38 a
	NO	1.25 ± 0.11 a	1.03 ± 0.06 a	0.71 ± 0.02 a	0.70 ± 0.01 a	0.25 ± 0.10 a	4.60 ± 0.97 a
	NNO	1.24 ± 0.08 b	1.02 ± 0.04 b	0.70 ± 0.05a	0.69 ± 0.04 a	0.22 ± 0.04 a	5.03 ± 0.59 a
21	Control	0.99 ± 0.02 a	0.83 ± 0.01 a	0.63 ± 0.01 a	0.76 ± 0.01 b	0.16 ± 0.01 a	5.13 ± 0.17 b
	NO	0.92 ± 0.04 b	0.78 ± 0.03 b	0.61 ± 0.02 a	0.78 ± 0.02 a	0.15 ± 0.01 b	5.36 ± 0.18 ab
	NNO	0.90 ± 0.04 b	0.76 ± 0.001 b	0.59 ± 0.00 b	0.78 ± 0.02 a	0.14 ± 0.01 b	5.50 ± 0.22 a

Note: Different letters within a column indicate statistically significant differences at $p < 0.05$ in Tukey's HSD test. Treatments: tap water (control), 20 mmol·L^{-1} NO_3^- (NO), and NO_3^- plus NO_2^- (NNO: 20 mmol·L^{-1} NO_3^- plus 100 μmol·L^{-1} NO_2^-). ABS/RC: absorption flux per PSII reaction center (RC), DIo/RC: dissipated energy flux per RC at $t = 0$, ETo/RC: electron transport flux per RC at $t = 0$, ETo/TRo: probability that a trapped exciton moves an electron into the electron transport chain beyond QA at $t = 0$, Fv/Fo: ratios characterizing the efficiency of PSII, TRo/RC: trapping flux leading to QA reduction per RC.

3.4. Transamination, free amino acid biosynthesis

In Exp. 1, foliar applications of NO and NNO caused significant increases in NR activity (Fig. A4B) and concentrations of NO_3^- (Fig. A4A) and free AAs (Fig. A4C) in the leaves.

In Exp. 2, foliar application of NNO100 induced upregulation of N metabolism, with significant increases in activities of NiR, GPT, and GOT and concentrations of the corresponding metabolites (Glu, Ala, and Asp). However, NNO300 treatment led to an inhibition of the activity of these metabolic enzymes, particularly GPT, which led to a significant decline in Ala concentration as compared with NNO100-treated leaves (Fig. 3). There was no significant difference in the percentage of Ala and Glu between the control and the leaves treated by NNO100, or NNO300 after 14 days (Fig. A5). Compared to the control, the percentage of the free AAs (Gln, Asp, Asn, and Arg) significantly increased and Phe, EtN, Trp, Ser, and Lys decreased in NNO100- and NNO300-treated leaves.

3.5. Polyamine concentrations and photochemical variables

NNO treatments resulted in significant declines in Put concentrations (by about 65%, $p = 0.01$) and photochemical parameters (ABS/RC by 9% and ETo/RC by 6%; $p < 0.05$) compared to the control values (Fig. 4A, D). A significant positive correlation between Put concentration and the photochemical index (Fv/Fo) was found in NNO-treated leaves ($r = 0.70$, $p = 0.02$; Fig. A6). NNO100 treatment caused an increase in chlorophyll index (by 8%, $p = 0.01$), but had no impact on Spd and Spm concentrations. NNO300 treatment led to a decline in Spm concentration (by 53%, $p = 0.01$) compared to NNO100-treated leaves (Fig. 4B).

3.6. Tricarboxylic acid cycle, total sugars, and free fatty acids

NNO treatments caused significant increases in the percentage of OAA and CA and decreases in SA, FA, and MA (Fig. 5A). Concentrations of TSs and free FAs were higher in NNO100- and NNO300-treated leaves than in the control (Fig. 5B and C). There were no significant differences in the percentage of TCA-related organic acids or concentrations of free FAs and TSs between NNO100- and NNO300-treated leaves.

3.7. Metabolite transport via the phloem

Compared to the control, NNO100 treatment significantly increased

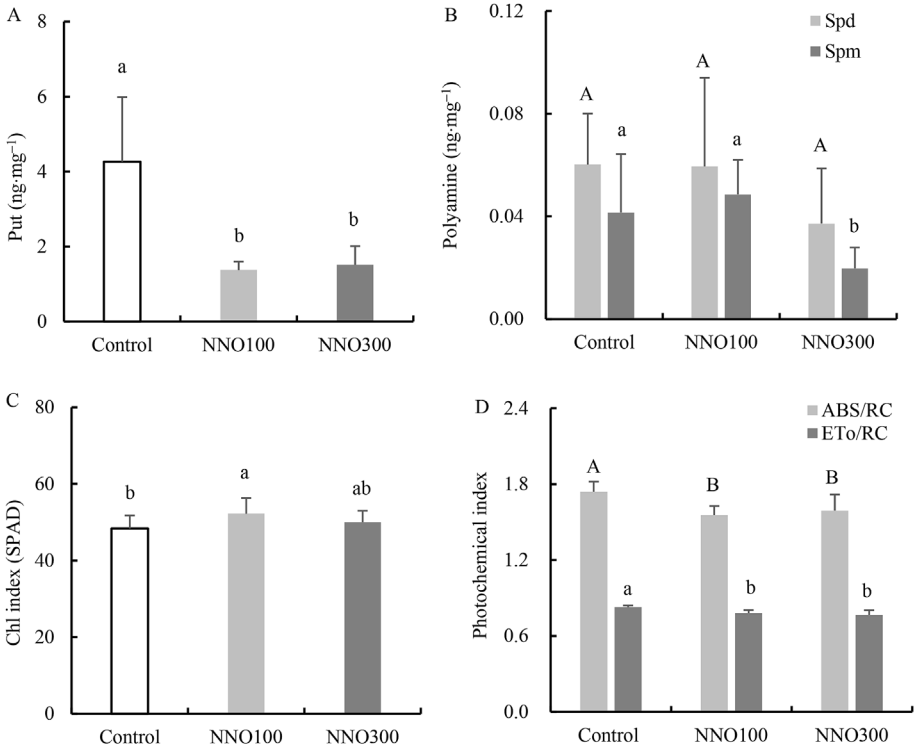

Fig. 4. Concentrations of putrescine (Put; A) and polyamines (Spd: spermidine, Spm: spermine; B), chlorophyll index (Chl, SPAD value; C), and photochemical efficiency (D) of leaves from 2-year-old poplar seedlings (*P. alba* × *P. berolinensis*) after 14 days of foliar spraying with tap water (Control), and NO_3^- plus NO_2^- solutions (NNO100: 20 mmol·L^{-1} NO_3^- plus 100 μmol·L^{-1} NO_2^-, NNO300: 20 mmol·L^{-1} NO_3^- plus 300 μmol·L^{-1} NO_2^-) (means ± SD, $n = 4$ for polyamine and photochemical parameters; n = 10 for Chl). ABS/RC: absorption flux per PSII reaction center (RC), ETo/RC: electron transport flux per RC at $t = 0$. Different letters above the columns indicate statistically significant differences among means at $p < 0.05$ by Tukey's HSD test.

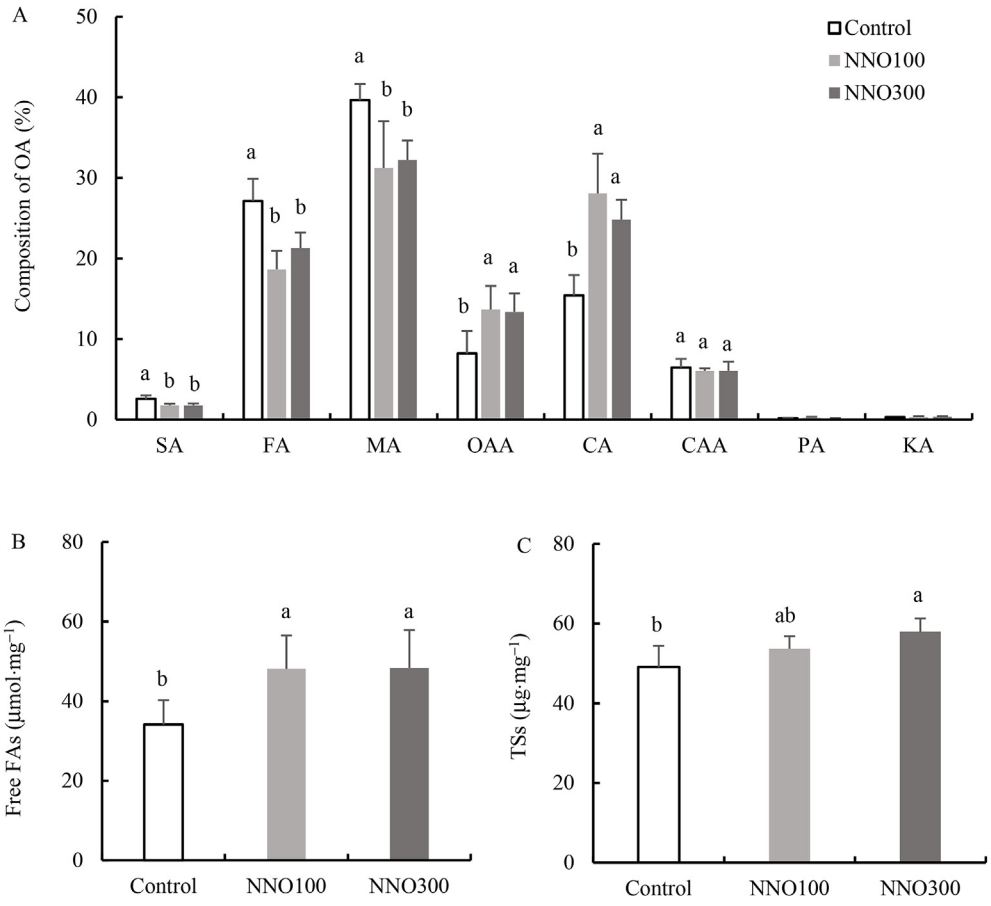

Fig. 5. (A) Composition of organic acids (%, OAs) in tricarboxylic acid cycle (TCA) and (B, C) concentrations of free fatty acids (free FAs) and total sugars (TSs) of leaves from 2-year-old poplar seedlings (*P. alba* × *P. berolinensis*) after 14 days of foliar spraying with tap water (Control), and NO_3^- plus NO_2^- solutions (NNO100: 20 mmol·L^{-1} NO_3^- plus 100 μmol·L^{-1} NO_2^-, NNO300: 20 mmol·L^{-1} NO_3^- plus 300 μmol·L^{-1} NO_2^-) (means ± SD, $n = 4$). Different letters above the columns indicate statistically significant differences among means at $p < 0.05$ by Tukey's HSD test.

total free AAs concentration in leaves and stem bark (phloem) (Fig. 6A); NNO300 treatment was inhibitory to petiole transport of free AAs, as indicated by declines in free AAs concentrations in the petiole and phloem. SS concentrations in leaves, petiole, or phloem did not differ significantly between the control and NNO100- or NNO300-treated plants.

4. Discussion

4.1. Mixed N treatments modified leaf surface properties

Uptake by roots is typically the primary N-supply pathway for plant growth (Marschner, 2012); N uptake through leaves may account for a smaller proportion of total N uptake (Hu and Sun, 2010). However, the significance of such mechanisms for plant N balance is not fully understood (Bourgeois et al., 2019). An increase in atmospheric reactive N may stimulate N input into plants through leaves (Weibull et al., 1990; Xu and Xiao, 2017). NO_3^- may penetrate leaves through the cuticle (Schönherr, 2006; Eichert, 2013), following the process of diffusion of water and solutes (Fernández et al., 2017). The permeation rate of NO_3^- was found to be low (Stiegler et al., 2013); this may be linked to electrostatic interactions between negatively-charged cuticle functional groups and NO_3^- (Aponte and Baur, 2018). The addition of organosilicon surfactants can significantly increase NO_3^- permeation (Schönherr, 2006) likely due to improved wetting and solubilizing effects at least the cuticle level. In Exp. 1, foliar applications of NO or NNO stimulated the formation of Si-rich crystals, which were larger in diameter and more frequent than the crystals on the control (Fig. 1). Enhanced crystallization was mainly on the adaxial leaf surface, so it may be associated with cuticular penetration. Because the adaxial leaf surface of hybrid poplar has few stomata (Hu et al., 2014), solutes sprayed on the surface most likely enter the leaf through the cuticle (Schönherr, 2006). The N atomic percentage of the crystal surface was higher on leaves treated with NO or NNO than on control leaves (Table

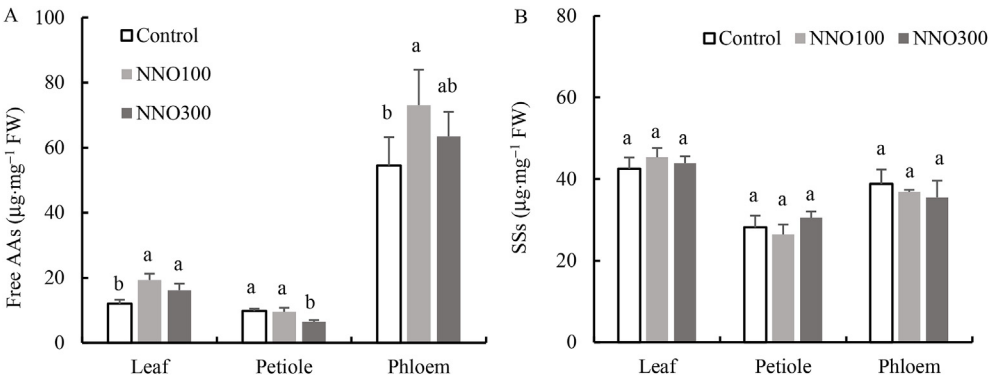

Fig. 6. Concentration of total free amino acids (AAs, A) of soluble sugars (SSs, B) of leaves, petioles, and stem bark (phloem) from 2-year-old poplar seedlings (*P. alba* × *P. berolinensis*) after 14 days of foliar spraying with tap water (Control), and NO_3^- plus NO_2^- solutions (NNO100: 20 mmol·L^{-1} NO_3^- plus 100 μmol·L^{-1} NO_2^-, NNO300: 20 mmol·L^{-1} NO_3^- plus 300 μmol·L^{-1} NO_2^-) (means ± SD, $n = 4$). Different letters above the same columns indicate statistically significant differences among means at $p < 0.05$ by Tukey's HSD test.

A1). Additionally, on the crystal surface of NNO-treated leaves, the atomic percentage of N was positively correlated with Si, but not on the control leaves (Fig. A2). This result suggests a potential link between the process of crystallization and exogenous N accumulation. This enhanced crystallization may be a potential pathway to alleviate the detrimental effects of NO or NNO on the leaves.

Relative to the cuticular penetration, the stomatal pathway is more important for solute uptake by leaves. In recent studies on intact leaves, uptake of mineral nutrients was greater through the stomata-bearing abaxial leaf surface than through the stomata-free adaxial surface (Eichert, 2013). The foliar uptake rate of the reactive N (such as nitrogen dioxide and peroxyacetyl nitrate) had a significant correlation with stomatal conductance (Chaparro-Suarez et al., 2011; Hu et al., 2015). In Exp. 1, some stomata and dense trichomes were observed on the abaxial leaf surface (Fig. A7); and stomata-related physiological variables (such as leaf Gs and E) did not differ significantly between the control and the leaves treated with NO or NNO. However, necrotic spots on the trichome surfaces were observed on treated leaves (Fig. A7), which implies that they were wettable. Recent studies have demonstrated significant roles of trichomes on wettability and foliar absorption (Li et al., 2018; Fernández and Bahamonde, 2019). Therefore, the dense "pubescence" of the abaxial leaf surface may be hydrophilic and have contributed to the applied N absorption. More specific trials will be however required for analyzing the foliar penetration pathways of poplar leaves in detail in future investigations.

4.2. Foliar N sprays induced qualitative and quantitative alterations of free amino acids and polyamines

In the studied poplar species, foliar applications of NO or NNO had no impact on N atomic percentage (At%) on the leaf surface (Table A1) or at mesophyll level as observed by SEM-EDX (data not shown). By contrast, foliar N sprays led to significant increases in leaf NO_3^- concentration, NR activity, and free AAs concentration (Fig. A4). Changes of the key N metabolic enzymes after N treatments have significant impacts on the process of N metabolism (Liu et al. 2016, 2018; Oliveira et al., 2017). Our results are consistent with the conclusions of Chen et al. (2014), who found that N deposited on *Populus cathayana* leaves was mainly assimilated as free AAs and soluble proteins, not cell-wall proteins. In the analysis of free AAs in Exp. 2, foliar N application (NNO100) induced concentration increases in most free AAs, with the highest increases in Glu, Gln, Asp, and Asn (Fig. A5). Enhanced synthesis of free AAs, particularly Gln and Asn, is considered an important indicator of increased N uptake (Vidmar et al., 2000; Xu and Xiao, 2017). An increase in foliar N input can impact NO_3^- uptake and transport of N metabolites in plant organs and tissues (Muller and Touraine, 1992). Moreover, the supply of AAs to the roots can also lead to an inhibition of root NO_3^- uptake (Dluzniewska et al., 2006). The inhibition of root NO_3^- uptake induced by free AAs may be a consequence of negative regulation of NO_3^- transporters (Vidmar et al., 2000). In Exp. 2, NNO100 treatment induced significant concentration increases in total free AAs in leaves and stem barks (phloem), but without a significant change of petiolar concentration. This result indicates that the N treatment stimulated free AAs export from leaves via the phloem. Our result agrees with that of Weibull et al. (1990), who found significant correlations between the amounts of the amino acids in leaf exudates and phloem sap. However, NNO300 treatment led to declines in concentrations of total free AAs in petioles ($p < 0.05$) and stem barks ($p = 0.16$). Perhaps NNO300 led to an inhibition of NiR activity (Fig. 3A), then to downregulation of N metabolism, particularly the synthesis of free AAs in the leaf and a decline in export via the phloem. In case of Jha et al. (2007), combined applications of NO_3^- and NO_2^- were significantly inhibitory to NR activity as compared to single NO_3^- treatment.

In addition, NNO300 treatment also led to significant declines in leaf concentrations of polyamines (Put and Spm) (Fig. 4A and B). Compared to Spd and Spm, Put seems to be more sensitive to mixed N treatments; because significant declines in leaf concentration of Put but not Spd and Spm occurred at NNO100 treatment. Putrescine in plant cells is biosynthesized through arginine decarboxylase (ADC)- and ornithine decarboxylase (ODC)-mediated pathways (Mattoo et al., 2010; Wu et al., 2016). Therefore, the leaf concentration of the precursors (Arg and Orn) or activity of the key enzymes (ADC or ODC) can be the factors affecting Put concentration (Gemperlová et al., 2006). In this study, a positive correlation between Put and Orn concentrations existed in the mixed N-treated leaves (Fig. A6A). Furthermore, declines in ODC activity were also found in the treated leaves (data not shown). NO_3^--induced declines in cellular Put concentration were also found in the poplar (*Populus nigra* × *maximoviczii*) (Minocha et al., 2004), which were accompanied with concentration increases of free Spd and Spm. Polyamines (Put, Spd, and Spm) are present in chloroplasts and photosynthetic subcomplexes (such as thylakoids, LHCII complex, and PSII membranes) (Kotzabasis et al., 1993; Bernet et al., 1999); they play important roles in maintaining chloroplast function and photochemical efficiency (Shu et al., 2012). In Exp. 2, leaf Put concentration is significantly positively correlated with the photochemical parameter (Fv/Fo) (Fig. A6B). Putrescine can impact the photochemical processes through regulations on photosystem II activity, photophosphorylation, and light energy dissipation (Ioannidis and Kotzabasis, 2007).

4.3. Mixed N treatments stimulated leaf transamination, dark respiration, and organic acid metabolism

N metabolism in plants is tightly coupled with C metabolism (Coruzzi and Zhou, 2001). For example, the biosynthesis of nitrogenous compounds (such as free AAs) depends on the availability of C to form the skeleton of the molecules. Maintaining an appropriate balance in C and N metabolism is crucial for optimal plant growth (Zhang et al., 2018). However, variations in the supply or metabolic status of one element (C or N) may substantially impact the metabolism of the other. For example, in transgenic *Arabidopsis thaliana* plants that expressed cyanobacterial fructose-1,6-bisphosphate and sedoheptulose-1,7-bisphosphatase in the chloroplasts, an increase in photosynthetic intermediates led to deficits of free AAs and a transient imbalance in the ratio of C to N in the leaves, which caused significant changes in the expression of the genes involved in the Calvin cycle and amino acid biosynthesis (Otori et al., 2017). NO_3^- or NO_2^- entering through leaves can result in a time-dependent inhibition of leaf net CO_2 assimilation (Foyer et al., 1994) and significant concomitant changes in the activity of the key enzymes phospho-enolpyruvate carboxylase and sucrose-phosphate synthase and photochemical processes (a decrease in quantum efficiency of PSII and an increase in non-radiative dissipation of excitation energy). Compared to NO_3^-, a low concentration of NO_2^- may have detrimental impacts on plant growth (Lee, 1979), through interference on C and N metabolism (Lange et al., 1989; Hu and Sun, 2010; Hu et al., 2014). For chloroplasts of some species, C fixation and oxygen production of the chloroplasts are less influenced by NO_3^-, but significantly inhibited by NO_2^- (Grant et al., 1972). In Exp. 1, NO or NNO treatment did not cause significant changes in net CO_2 assimilation, but led to declines in the quantum efficiency of PSII. On day 7 of foliar application of the NO_3^-/NO_2^- mixed solution, leaf dark respiration rate was significantly higher than in the control (R_{dark} did not change for 21 days) and NO_3^--treated leaves (R_{dark} increased through 21 days). In an early study by Birch et al. (1986), NO_3^- feeding resulted in a substantial increase in dark respiration. An analysis of organic acids in the TCA cycle in Exp. 2 showed that NNO100 or NNO300 treatment caused concentration increases of OAA and CA and decreases of SA and FA in the leaves. Free FAs concentration and transamination also increased (as indicated by significant increases in the activity of GPT and GOT and concentration of Ala and Asp). NNO-caused increase in dark respiration may be due to the mixed N application enhancing transamination from pyruvic acid to Ala and from oxaloacetic acid to Asp;

rapid consumptions of PA and OAA stimulate conversions of organic acids from SA and FA to OAA and CA; these changes may, in turn, cause an increase in respiration and free FAs metabolism through the TCA and fatty acid-coupling pathways (Rasmussen et al., 2008). Our results are consistent with the results reported by O'Leary et al. (2017), who found leaf R_{dark} rates were correlated positively with levels of the C and N metabolites, particularly with Ala, which has the most consistently strong correlation with leaf R_{dark} rate. Ala level in tissues is tightly linked with pyruvate level via Ala aminotransferase (O'Leary et al., 2017).

4.4. Foliar N applications changed the morphoanatomical traits and water status

Foliar applications of NO_3^--N or NO_2^--N at low concentrations can cause changes in physiological processes or leaf biomass but rarely visible injury (Wellburn, 1990). However, anatomical analyses have shown microscopic damage to epidermal and mesophyll cells of NO_3^--treated leaves before any macroscopic injury was visible (Bitterlich and Upadhyaya, 1990). In Exp. 1, microscopic crack or collapse on the adaxial leaf surface and macroscopic injury (marginal necrosis and curling) developed on leaves treated with NO- and NNO-treated plants. Moreover, NNO treatment led to a significant decline in leaf biomass ($p < 0.05$) compared to control and NO-treated leaves. The application variables of the simulated N solution (40 mL·plant^{-1}, once a day, NO_3^-/NO_2^- mixture) may have influenced the degree of injury observed but this need to be examined with more detail in future trials. Additionally, the role of pubescence on the abaxial leaf surfaces may increase solution retention (Bitterlich and Upadhyaya, 1990) but the physic-chemical properties of poplar leaves concerning foliar deposition and absorption of contaminants have to be assessed in future trials. Increased leaf temperature with decreased leaf hydraulic performance (water evaporation and conductance) can also result in significant changes in leaf morphoanatomical traits, even visible leaf injury (Monteiro et al., 2016). In Exp. 1, NO or NNO treatment caused significant increases in leaf temperature, but without significant changes in the leaf transpiration rate. Because the foliar application of NNO also led to significant decreases in AWC and WUE (Fig. A3), less water might have been taken up and transported. NO_3^- permeation of the cuticle might also increase leaf water loss by disturbing small pores in the cuticle (Bowman and Paul, 1990). In addition, the decline of energy dissipation observed in the treated leaves (Table 1) would aggravate damage to a leaf, particularly at the margins when temperature and irradiance are highest because the temperature at the margins is commonly higher than at the central area of a leaf under stress (Takeuchi et al., 2016).

5. Conclusion

Physiological investigations with visual assessments are essential to evaluate the actual effects of simulated acid deposition. Significant changes in leaf morphoanatomical traits and physiological processes occurred in the hybrid poplar treated by NO or NNO. Visible leaf injuries and enrichment of Si-rich crystals on the adaxial leaf surface were obvious on N treated leaves. However, it is uncertain whether the crystallization process is involved in cuticle permeation (that is, as a potential pathway of solute entry) or as a detoxification process (exogenous N incorporation into the crystals may potentially alleviate injury on the leaf surface). Poplar leaves are more sensitive to NO_2^- even at the applied low concentration; because significant declines in water content and dry mass were found only in NNO-treated leaves. Moreover, NNO applications induced increases in transamination (increasing activities of GOT and GPT) and free AAs biosynthesis in leaves, altering the TCA cycle, dark respiration, and N transport via the phloem. It is noted that a higher NO_2^- concentration (300 μmol·L^{-1}) in the mixed solution can inhibit polyamine metabolism, the activity of key N-metabolic enzymes and N transport via the phloem; however, the underlying mechanisms are unclear and require further investigation. In addition to the physiological and metabolic effects of atmospheric pollutants, future studies should focus on examining potential roles of leaf surface structure, composition, and function concerning foliar absorption and transport of N species in tree plants.

Conflicts of interest

The authors hereby declare no conflicts of interests.

Author contributions

Yanbo Hu and Andreas D. Peuke conceived the experiments; Yanbo Hu analyzed the data and wrote the main manuscript; Yanbo Hu, Xiyang Zhao, Junxin Yan, and Chunming Li performed the experiments; and Andreas D. Peuke provided constructive discussions.

Acknowledgements

The study was financially supported by the National Key Research and Development Program of China (Grant No. 2016YFD0600404); Fundamental Research Funds for the Central Universities (Grant No. 2572019BD06); Open Fund from Key Laboratory of Saline-alkali Vegetation Ecology Restoration, Ministry of Education (Grant No. SAVER1801); National Natural Science Foundation of China (Grant No. 31300506). We thank Dr. Victoria Fernández (Technical University of Madrid, Spain) for critical reading and Dr. Beth E. Hazen (Willows End Scientific Editing and Writing) for manuscript editing.

Appendix

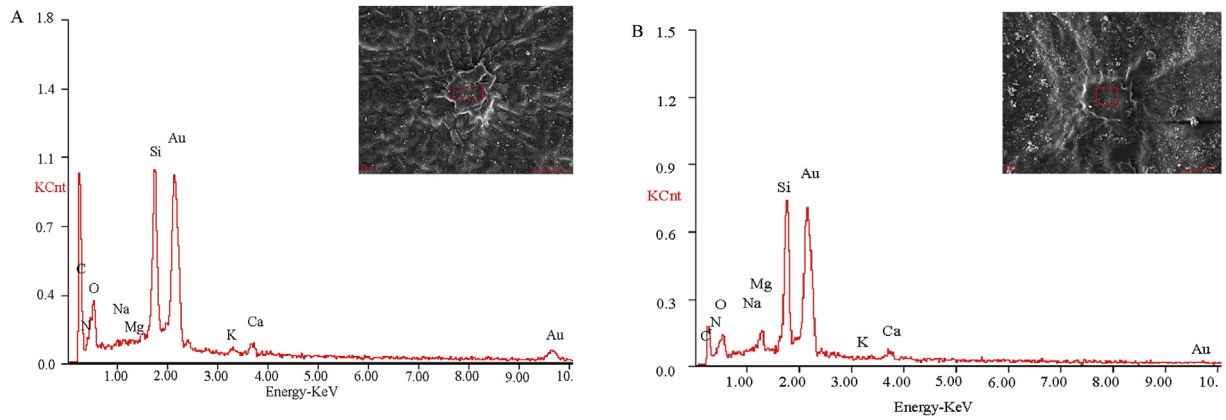

Fig. A1. Energy dispersive X-Ray analysis of elements in crystals on the adaxial leaf surface of poplar seedlings after 21 days of daily sprays with tap water (control, A) and NO_3^-/NO_2^- mixture (20 mmol·L^{-1} NO_3^- and 100 μmol·L^{-1} NO_2^-, B). Results showed that the crystals are silicon-rich compounds.

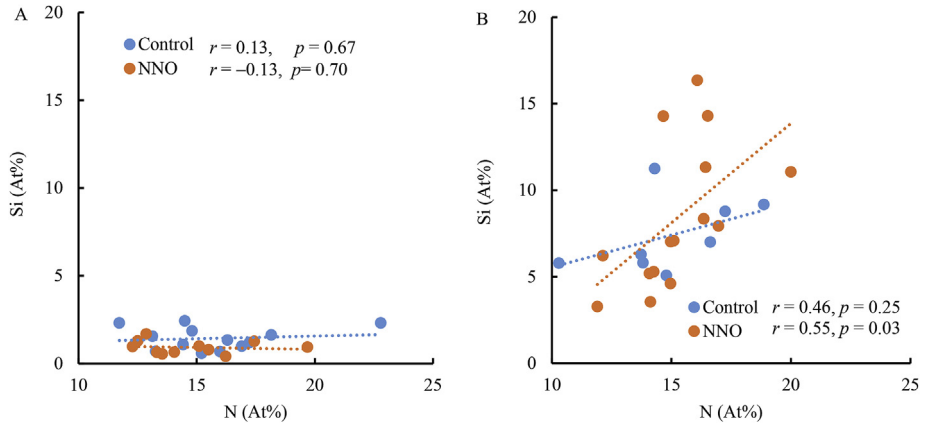

Fig. A2. Correlation analysis between Si and N atomic percentage (At%) on the non-crystal (A) and crystal (B) areas of the surface of leaves from 2-year-old poplar seedlings (*Populus alba* × *P. berolinensis*) after 21 days of foliar spraying with tap water (control) and NO_3^- plus NO_2^- solution (NNO: 20 mmol·L^{-1} NO_3^- plus 100 μmol·L^{-1} NO_2^-). The Pearson correlation coefficient (r) and linear regression analysis were used; statistical significance ($p < 0.05$) of the model and the regression coefficient was verified by *F*-test and Student's *t*-test, respectively.

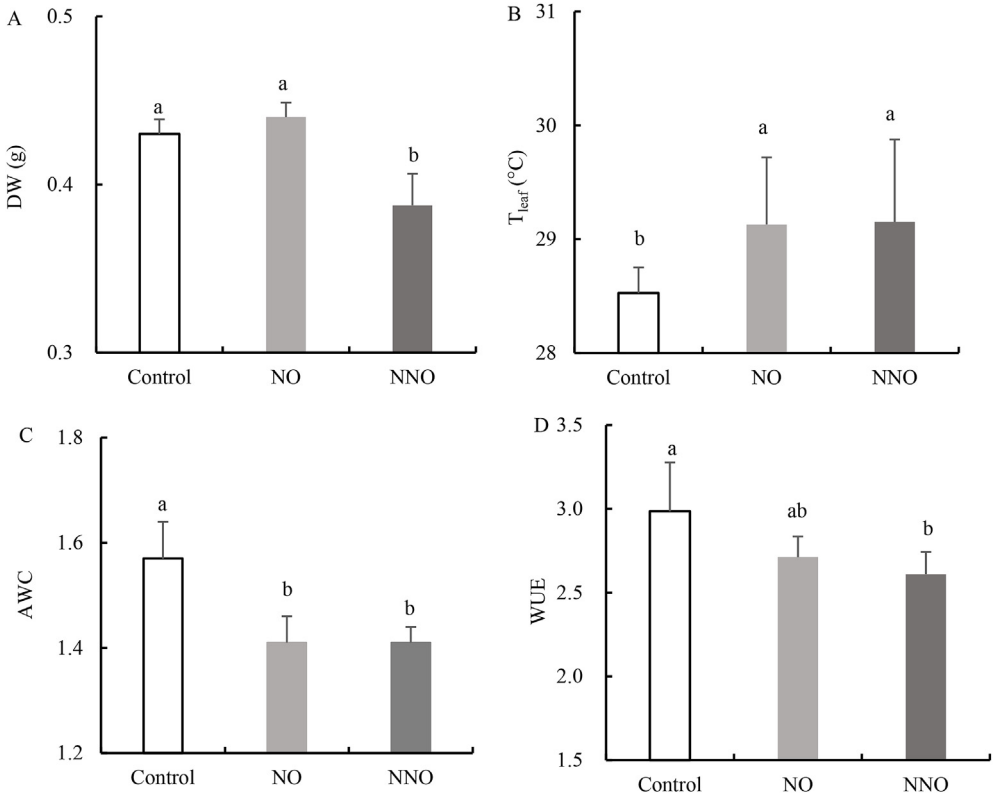

Fig. A3. Dry weight (DW, A), surface temperature (T_{leaf}, B), absolute water content (AWC, C), and water-use efficiency (WUE, D) of leaves from 2-year-old poplar seedlings (*P. alba* × *P. berolinensis*) after 21 days of foliar spraying with tap water (control), NO_3^- solution (NO: 20 mmol·L^{-1}), and NO_3^- plus NO_2^- solution (NNO: 20 mmol·L^{-1} NO_3^- plus 100 μmol·L^{-1} NO_2^-) (mean ± SD; $n = 6$). Different letters above the columns indicate statistically significant differences among means at $p < 0.05$ by Tukey's HSD test.

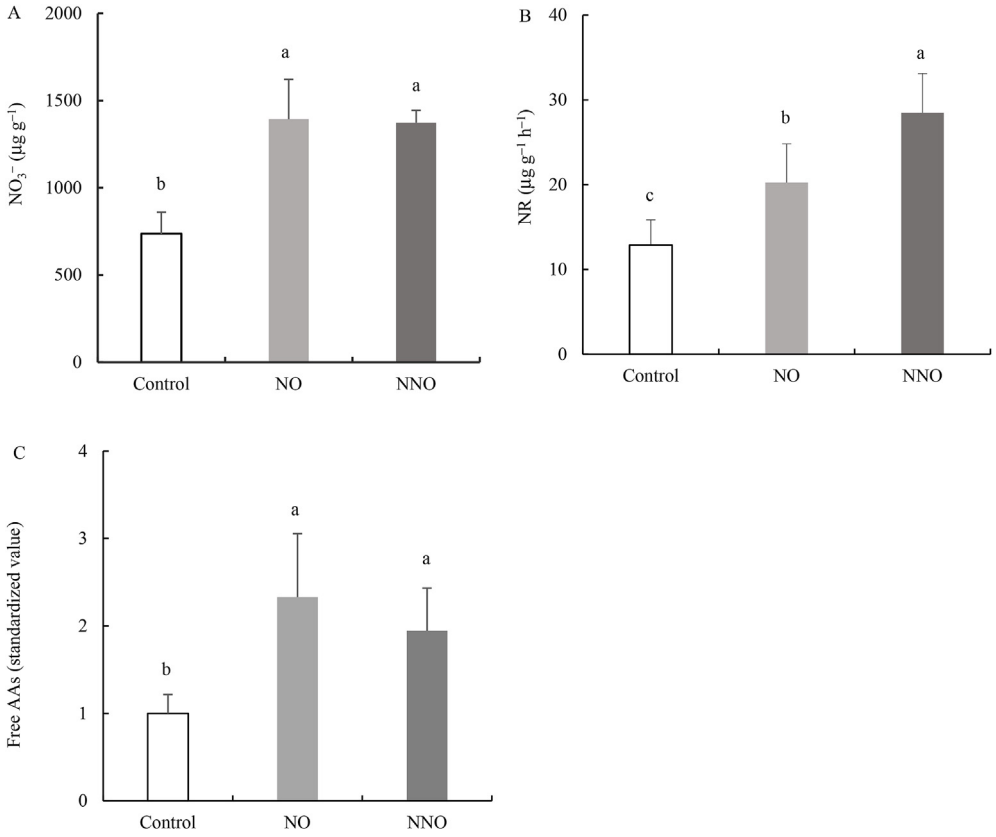

Fig. A4. Nitrate (NO_3^-) concentration (A), nitrate reductase (NR) activity (B), and free amino acid (Free AAs) concentration (C) of leaves from 2-year-old poplar seedlings (*P. alba* × *P. berolinensis*) after 21 days of foliar spraying with tap water (control), NO_3^- solution (NO: 20 mmol·L^{-1}), and NO_3^- plus NO_2^- solution (NNO:

20 mmol·L^{-1} NO_3^- plus 100 μmol·L^{-1} NO_2^-) (means ± SD, $n = 4$). Different letters above the columns indicate statistically significant differences among means at $p < 0.05$ by Tukey's HSD test.

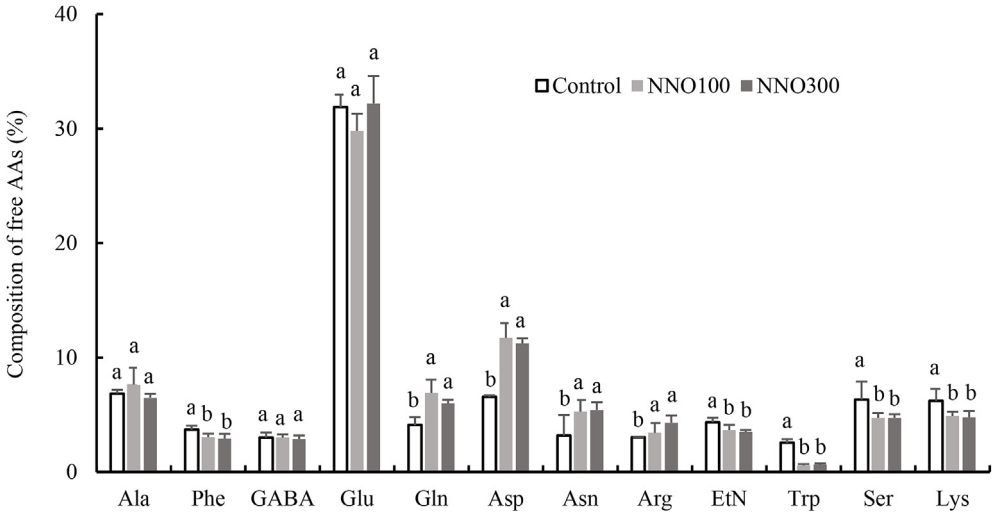

Fig. A5. Composition of free amino acids (%, free AAs) in leaves of 2-year-old poplar seedlings (*P. alba* × *P. berolinensis*) after 14 days of foliar spraying with tap water (Control), and NO_3^- plus NO_2^- solutions (NNO100: 20 mmol·L^{-1} NO_3^- plus 100 μmol·L^{-1} NO_2^-, NNO300: 20 mmol·L^{-1} NO_3^- plus 300 μmol·L^{-1} NO_2^-) (means ± SD, $n = 4$). Different letters above the columns indicate statistically significant differences among means at $p < 0.05$ by Tukey's HSD test.

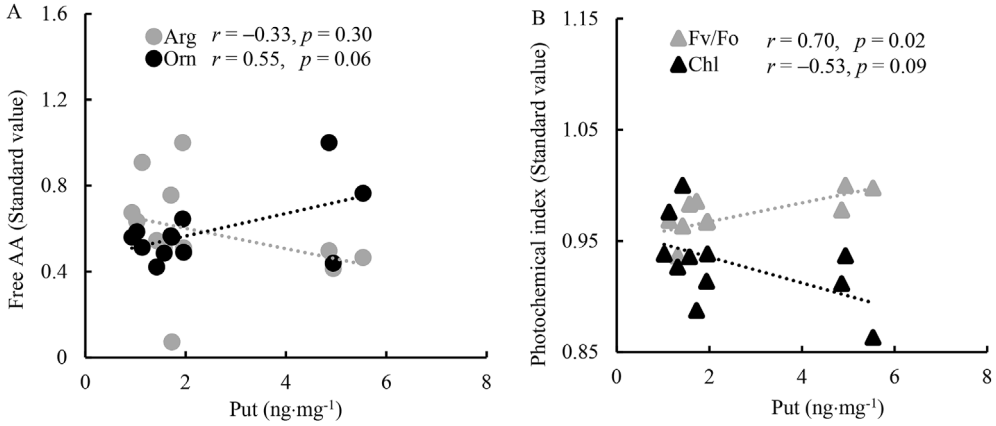

Fig. A6. Correlation analysis of putrescine concentration with free AA (Arg and Orn; A), and with photochemical indexes (Fv/Fo and Chl concentration; B) of leaves from 2-year-old poplar seedlings (*Populus alba* × *P. berolinensis*) after 14 days of foliar spraying with tap water and NO_3^- plus NO_2^- solutions. The Pearson correlation coefficient (r) and linear regression analysis were used; statistical significance ($p < 0.05$) of the model and the regression coefficient was verified by F-test and Student's t-test, respectively.

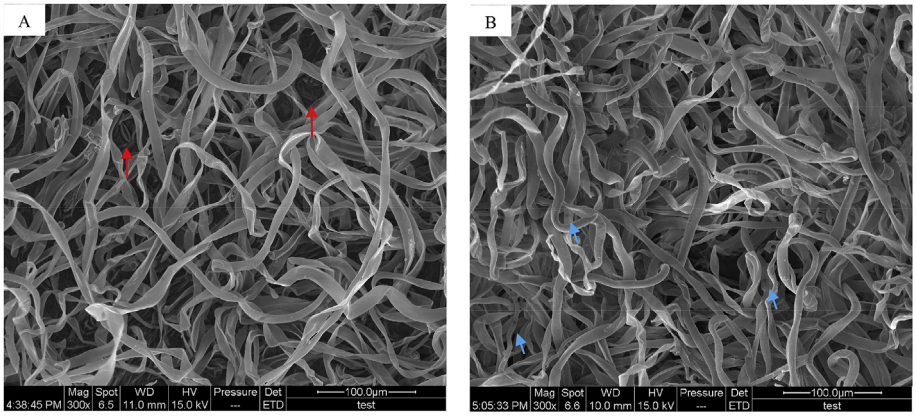

Fig. A7. Dense trichomes on the abaxial surface of poplar leaves after 21 days of daily sprays with tap water (control, A) or NO_3^-/NO_2^- mixture (20 mmol·L^{-1} NO_3^- and 100 μmol·L^{-1} NO_2^-, B). Red arrows: stomata, blue arrows: necrotic spots.

Table A1

Atomic percentage (At%) of chemical elements on the non-crystal and crystal areas on the adaxial surface of fully-expanded leaves of 2-year-old poplar seedlings (*Populus alba* × *P. berolinensis*) sprayed daily with tap water (control), 20 mmol·L^{-1} NO_3^- (NO) and NO_3^- plus NO_2^- (NNO: 20 mmol·L^{-1} NO_3^- plus 100 μmol·L^{-1} NO_2^-) for 21 days (mean ± SD, $n = 6$).

Surface	Treatment	C	N	O	Na	Mg	Si	K	Ca
Non-crystal	Control	68.64 ± 3.48 a	14.88 ± 1.89 a	13.64 ± 2.25 c	0.16 ± 0.14 a	0.24 ± 0.13 b	1.60 ± 0.55 b	0.43 ± 0.12 a	0.42 ± 0.13 b
	NO	70.80 ± 3.06 a	14.65 ± 1.73 a	12.14 ± 1.26 c	0.15 ± 0.09 a	0.19 ± 0.09 b	1.26 ± 0.78 b	0.36 ± 0.15 ab	0.45 ± 1.67 b
	NNO	70.58 ± 5.44 a	13.99 ± 2.05 a	13.27 ± 3.42 c	0.16 ± 0.18 a	0.22 ± 0.08 b	1.11 ± 0.38 b	0.25 ± 0.10 b	0.42 ± 0.11 b
Crystal	Control	64.52 ± 6.30 ab	14.31 ± 2.07 a	12.48 ± 4.14 c	0.23 ± 0.09 a	0.53 ± 0.58 b	6.78 ± 2.24 a	0.33 ± 0.21 ab	0.82 ± 0.30 a
	NO	58.57 ± 5.78 b	14.60 ± 1.49 a	14.43 ± 4.94 b	0.30 ± 0.24 a	1.20 ± 1.54 ab	9.98 ± 4.22 a	0.26 ± 0.07 b	0.90 ± 0.75 a
	NNO	51.40 ± 8.91 c	16.01 ± 1.83 a	20.03 ± 4.62 a	0.25 ± 0.15a	1.61 ± 1.18 a	9.43 ± 4.07 a	0.25 ± 0.13 b	1.01 ± 0.67 a

Note: Different letters within a column indicate statistically significant differences at $p < 0.05$ in Tukey's HSD test.

References

Aponte, J., Baur, P., 2018. The role of pH for ionic solute uptake by the non-aerial hypocotyl of mung bean plants. J. Plant Dis. Prot. 125 (4), 433–442.

Bernet, E., Claparols, I., Dondini, L., Santos, M.A., Serafini-Fracassini, D., Torné, J.M., 1999. Changes in polyamine content, arginine and ornithine decarboxylases and transglutaminase activities during light/dark phases (of initial differentiation) in maize calluses and their chloroplasts. Plant Physiol. Biochem. 37, 899–909.

Birch, D.G., Elrifi, I.R., Turpin, D.H., 1986. Nitrate and ammonium induced photosynthetic suppression in N-limited *Selenastrum minutum*. II. Effects of NO_3^- and NH_4^+ addition on CO_2 efflux in the light. Plant Physiol. 82, 708–712.

Bitterlich, I., Upadhyaya, M.K., 1990. Leaf surface ultrastructure and susceptibility to ammonium nitrate injury. Can. J. Bot. 68 (9), 1911–1915.

Bourgeois, I., Clément, J.C., Caillon, N., Savarino, J., 2019. Foliar uptake of atmospheric nitrate by two dominant subalpine plants: insights from in situ triple-isotope analysis. New Phytol. 223 (4), 1784–1794.

Bowman, D.C., Paul, J.L., 1990. The foliar absorption of urea-N by tall fescue and creeping bentgrass turf. J. Plant Nutr. 13 (9), 1095–1113.

Chaparro-Suarez, I.G., Meixner, F.X., Kesselmeier, J., 2011. Nitrogen dioxide (NO_2) uptake by vegetation controlled by atmospheric concentrations and plant stomatal aperture. Atmos. Environ. 45 (32), 5742–5750.

Chen, F.J., Lao, Q.B., Jia, G.D., Chen, C.Q., Zhu, Q.M., Zhou, X., 2019. Seasonal variations of nitrate dual isotopes in wet deposition in a tropical city in China. Atmos. Environ. 196, 1–9.

Chen, L.H., Dong, T.F., Duan, B.L., 2014. Sex-specific carbon and nitrogen partitioning under N deposition in *Populus cathayana*. Trees (Berl.) 28, 793–806.

Coruzzi, G.M., Zhou, L., 2001. Carbon and nitrogen sensing and signaling in plants: emerging 'matrix effects'. Curr. Opin. Plant Biol. 4, 247–253.

Dluzniewska, P., Gessler, A., Kopriva, S., Strnad, M., Novák, O., Dietrich, H., Rennenberg, H., 2006. Exogenous supply of glutamine and active cytokinin to the roots reduces NO_3^- uptake rates in poplar. Plant Cell Environ. 29 (7), 1284–1297.

Eichert, T., 2013. Foliar nutrient uptake of myths and legends. Acta Hortic. (Wagening.) (984), 69–75.

Elvir, J.A., Wiersma, G.B., Day, M.E., Greenwood, M.S., Fernandez, I.J., 2006. Effects of enhanced nitrogen deposition on foliar chemistry and physiological processes of forest trees at the Bear Brook Watershed in Maine. For. Ecol. Manag. 221, 207–214.

Fernández, V., Bahamonde, H.A., 2019. Advances in foliar fertilizers to optimize crop nutrition. In: Rengel, Z. (Ed.), Achieving Sustainable Crop Nutrition. Burleigh Dodds Science Publishing Limited, UK (in press). doi:10.19103/AS.2019.0062.29.

Fernández, V., Bahamonde, H.A., Peguero-Pina, J.J., Gil-Pelegrín, E., Sancho-Knapik, D., Goldbach, H.E., Gil, L., Eichert, T., 2017. Physico-chemical properties of plant cuticles and their functional and ecological significance. J. Exp. Bot. 68 (19), 5293–5306.

Foyer, C.H., Noctor, G., Lelandais, M., Lescure, J.C., Valadier, M.H., Boutin, J.P., Horton, P., 1994. Short-term effects of nitrate, nitrite and ammonium assimilation on photosynthesis, carbon partitioning and protein phosphorylation in maize. Planta 192, 211–220.

Gao, G., Clare, A.S., Rose, C., Caldwell, G.S., 2017. Reproductive sterility increases the capacity to exploit the green seaweed *Ulva rigida* for commercial applications. Algal Res 24, 64–71.

Gemperlová, L., Nováková, M., Vaňková, R., Cvikrová, J.E.M., 2006. Diurnal changes in polyamine content, arginine and ornithine decarboxylase, and diamine oxidase in tobacco leaves. J. Exp. Bot. 57 (6), 1413–1421.

Ghashghaie, J., Brenckmann, F., Saugier, B., 1992. Water relations and growth of rose plants cultured in vitro under various relative humidities. Plant Cell Tiss. Org. 30 (1), 51–57.

Grant, B.R., Winkenbach, F., Canvin, D.T., Bidwell, R.G.S., 1972. The effect of nitrate, nitrite, and ammonia on photosynthesis by *Acetabularia* chloroplast preparations compared with spinach chloroplasts and whole cells of *Acetabularia* and *Dunaliella*. Can. J. Bot. 50 (12), 2535–2543.

Harbin Water Supply Group Co. Ltd, 2018. Water Quality Report 2018(08): 42 Physical and Chemical Index of Tap Water. . http://www.hrbgongshui.com/content/?1341.html, Accessed date: 20 October 2018.

Hayashi, K., Komada, M., Miyata, A., 2007. Atmospheric deposition of reactive nitrogen on turf grassland in central Japan: comparison of the contribution of wet and dry deposition. Water, Air, Soil Pollut. 7 (1–3), 119–129.

Hu, Y.B., Bellaloui, N., Sun, G.Y., Wang, J.H., 2014. Exogenous sodium sulfide improves morphological and physiological responses of a hybrid *Populus* species to nitrogen dioxide. J. Plant Physiol. 171 (10), 868–875.

Hu, Y.B., Bellaloui, N., Tigabu, M., Wang, J.H., Diao, J., Wang, K., Yang, R., 2015. Gaseous NO_2 effects on stomatal behavior, photosynthesis and respiration of hybrid poplar leaves. Acta Physiol. Plant. 37, 39. https://doi.org/10.1007/s11738-014-1749-8.

Hu, Y.B., Fernández, V., Ma, L., 2014. Nitrate transporters in leaves and their potential roles in foliar uptake of nitrogen dioxide. Front. Plant Sci. 5, 360. https://doi.org/10.3389/fpls.2014.00360.

Hu, Y.B., Sun, G.Y., 2010. Leaf nitrogen dioxide uptake coupling apoplastic chemistry, carbon/sulfur assimilation, and plant nitrogen status. Plant Cell Rep. 29 (10), 1069–1077.

Ioannidis, N.E., Kotzabasis, K., 2007. Effects of polyamines on the functionality of photosynthetic membrane in vivo and in vitro. Biochim. Biophys. Acta 1767, 1372–1382.

Jha, P., Ali, A., Raghuram, N., 2007. Nitrate-induction of nitrate reductase and its inhibition by nitrite and ammonium ions in *spirulina platensis*. Physiol. Mol. Biol. Plants 13 (2), 163–167.

Jin, X.H., Huang, H., Wang, L., Sun, Y., Dai, S.L., 2016. Transcriptomics and metabolite analysis reveals the molecular mechanism of anthocyanin biosynthesis branch pathway in different *Senecio cruentus* cultivars. Front. Plant Sci. 7, 1307.

Kannan, S., Charnel, A., 1986. Foliar absorption and transport of inorganic nutrients. Crit. Rev. Plant Sci. 4 (4), 341–375.

Karnosky, D.F., Gagnon, Z.E., Reed, D.D., Witter, J.A., 1992. Effects of genotype on the response of *Populus tremuloides* michx. to ozone and nitrogen deposition. Water, Air, Soil Pollut. 62 (3–4), 189–199.

Kotzabasis, K., Fotinou, C., Roubelakis-Angelakis, K.A., Ghanotakis, D., 1993. Polyamines in the photosynthetic apparatus: photosystem H highly resolved subcomplexes are enriched in spermine. Photosynth. Res. 38, 83–88.

Lange, O.L., Heber, U., Schulze, E.D., Ziegler, H., 1989. Atmospheric pollutants and plant metabolism. In: In: Schulze, E.D., Lange, O.L., Oren, R. (Eds.), Forest Decline and Air Pollution, Ecological Studies, vol. 77. Springer, Berlin Heidelberg New York, pp. 238–273.

Lee, R.B., 1979. The effect of nitrite on root growth of barley and maize. New Phytol. 83 (3), 615–622.

Li, C., Wang, P., Lombi, E., Wu, J., Blamey, F.P.C., Fernández, V., Howard, D.L., Menzies, N.W., Kopittke, P.M., 2018. Absorption of foliar applied Zn is decreased in Zn deficient sunflower (*Helianthus annuus*) due to changes in leaf properties. Plant Soil 433 (1–2), 309–322.

Liao, Y.C., Fan, H.B., Li, Y.Y., Liu, W.F., Yuan, Y.H., 2010. Effects of simulated nitrogen deposition on growth and photosynthesis of 1-year-old Chinese fir (*Cunninghamia lanceolata*) seedlings. Acta Ecol. Sin. 30 (3), 150–154.

Liu, B.Y., Lei, C.Y., Jin, J.H., Guan, Y.Y., Li, S., Zhang, Y.S., Liu, W.Q., 2016. Physiological responses of two moss species to the combined stress of water deficit and elevated N deposition (II): carbon and nitrogen metabolism. Ecol. Evol. 6, 7596–7609.

Liu, N., Wu, S.H., Guo, Q.F., Wang, J.X., Cao, C., Wang, J., 2018. Leaf nitrogen assimilation and partitioning differ among subtropical forest plants in response to canopy addition of nitrogen treatments. Sci. Total Environ. 637–638, 1026–1034.

Liu, X.J., Duan, L., Mo, J.M., Du, E.Z., Shen, J.L., Lu, X.K., Zhang, Y., Zhou, X.B., He, C.E., Zhang, F.S., 2011. Nitrogen deposition and its ecological impact in China: an overview. Environ. Pollut. 159 (10), 2251–2264.

Manninen, S., Woods, C., Leith, I.D., Sheppard, L.J., 2011. Physiological and morphological effects of long-term ammonium or nitrate deposition on the green and red (shade and open grown) *Sphagnum capillifolium*. Environ. Exp. Bot. 72, 140–148.

Mao, Q.G., Lu, X.K., Mo, H., Gundersen, P., Mo, J.M., 2018. Effects of simulated N deposition on foliar nutrient status, N metabolism and photosynthetic capacity of three dominant understory plant species in a mature tropical forest. Sci. Total Environ. 610–611, 555–562.

Marschner, P., 2012. Marschner's Mineral Nutrition of Higher Plants, third ed. Academic Press, London, pp. 672. https://doi.org/10.1016/C2009-0-63043-9.

Masclaux-Daubresse, C., Daniel-Vedele, F., Chardon, J.D.F., Gaufichon, L., Suzuki, A., 2010. Nitrogen uptake, assimilation and remobilization in plants: challenges for sustainable and productive agriculture. Ann. Bot. 105 (7), 1141–1157.

Mattoo, A.K., Minocha, S.C., Minocha, R., Handa, A.K., 2010. Polyamines and cellular metabolism in plants: transgenic approaches reveal different responses to diamine putrescine versus higher polyamines spermidine and spermine. Amino Acids 38, 405–413.

Minocha, R., Lee, J.S., Long, S., Bhatnagar, P., Minocha, S.C., 2004. Physiological responses of wild type and putrescine-overproducing transgenic cells of poplar to

variations in the form and concentration of nitrogen in the medium. Tree Physiol. 24 (5), 551–560.
Minocha, R., Long, S., Magill, A.H., Aber, J., McDowell, W.H., 2000. Foliar free polyamine and inorganic ion content in relation to soil and soil solution chemistry in two fertilized forest stands at the Harvard Forest, Massachusetts. Plant Soil 222 (1), 119–137.
Monteiro, M.V., Blanusa, T., Verhoef, A., Hadley, P., Cameron, R.W.F., 2016. Relative importance of transpiration rate and leaf morphological traits for the regulation of leaf temperature. Aust. J. Bot. 64 (1), 32–44.
Muller, B., Touraine, B., 1992. Inhibition of NO_3^- uptake by various phloem-translocated amino acids in soybean seedlings. J. Exp. Bot. 43, 617–623.
O'Leary, B.M., Lee, C.P., Atkin, O.K., Cheng, R., Brown, T.B., Harvey, M.A., 2017. Variation in leaf respiration rates at night correlates with carbohydrate and amino acid supply. Plant Physiol. 174, 2261–2273.
Oliveira, H.C., da Silva, L.M.I., de Freitas, L.D., Debiasi, T.V., Marchiori, N.M., Aidar, M.P.M., Bianchini, E., Pimenta, J.A., Stolf-Moreira, R., 2017. Nitrogen use strategies of seedlings from neotropical tree species of distinct successional groups. Plant Physiol. Biochem. 114, 119–127.
Otori, K., Tanabe, N., Maruyama, T., Sato, S., Yanagisawa, S., Tamoi, M., Shigeoka, S., 2017. Enhanced photosynthetic capacity increases nitrogen metabolism through the coordinated regulation of carbon and nitrogen assimilation in *Arabidopsis thaliana*. J. Plant Res. 130 (5), 909–927.
Payne, R.J., Dise, N.B., Stevens, C.J., Gowing, D.J., Partners, B., 2013. Impact of nitrogen deposition at the species level. Proc. Natl. Acad. Sci. 110 (3), 984–987.
Peuke, A.D., Jeschke, W.D., Hartung, W., 1998b. Foliar application of nitrate or ammonium as sole nitrogen supply in *Ricinus communis* II. The flows of cations, chloride and abscisic acid. New Phytol. 140, 625–636.
Peuke, A.D., Jeschke, W.D., Dietz, K.J., Schreiber, L., Hartung, W., 1998a. Foliar application of nitrate or ammonium as sole nitrogen supply in *Ricinus communis* I. Carbon and nitrogen uptake and inflows. New Phytol. 138 (4), 675–687.
Rasmussen, S., Parsons, A.J., Fraser, K., Xue, H., Newman, J.A., 2008. Metabolic profiles of *Lolium perenne* are differentially affected by nitrogen supply, carbohydrate content, and fungal endophyte infection. Plant Physiol. 146, 1440–1453.
Rennenberg, H., Wildhagen, H., Ehlting, B., 2010. Nitrogen nutrition of poplar trees. Plant Biol. 12, 275–291.
Sant'Anna-Santos, B.F., da Silva, L.C., Azevedo, A.A., Aguiar, R., 2006. Effects of simulated acid rain on leaf anatomy and micromorphology of *Genipa americana* L. (*Rubiaceae*). Braz. Arch. Biol. Technol. 49 (2), 313–321.
Schönherr, J., 2006. Characterization of aqueous pores in plant cuticles and permeation of ionic solutes. J. Exp. Bot. 57 (11), 2471–2491.
Shah, I., Petroczi, A., James, R.A., Naughton, D.P., 2013. Determination of nitrate and nitrite content of dietary supplements using ion chromatography. J. Anal. Bioanal. Tech. S12, 1–7.
Shu, S., Guo, S.R., Yuan, L.Y., 2012. A review: polyamines and photosynthesis. In: Advances in Photosynthesis-Fundamental Aspects InTech. Open Access Publisher, Croatia, pp. 439–464.
Singh, J.P., Singh, J.N., 1978. Effect of nitrate on respiration of *Mentha arvensis*. Biol. Plant. 20 (6), 403–408.
Song, J.J., Nada, K., Tachibana, S., 2001. The early increase of S-adenosylmethionine decarboxylase activity is essential for the normal germination and tube growth in tomato (*Lycopersicon esculentum* Mill.) pollen. Plant Sci. 161 (3), 507–515.
Stevens, C.J., David, T.I., Storkey, J., 2018. Atmospheric nitrogen deposition in terrestrial ecosystems: its impact on plant communities and consequences across trophic levels. Funct. Ecol. 32, 1757–1769.
Stiegler, J.C., Richardson, M.D., Karcher, D.E., Roberts, T.L., Norman, R.J., 2013. Foliar absorption of various inorganic and organic nitrogen sources by creeping bentgrass. Crop Sci. 53, 1148–1152.
Streeter, J.G., Bosler, M.E., 1972. Comparison of in vitro and in vivo assays for nitrate reductase in soybean leaves. Plant Physiol. 49, 448–450.
Su, T., Han, M., Min, J., Cao, D., Zhai, G.Q., Zhou, H.Y., Li, N.Y., Li, M.Z., 2019. Genome-wide characterization of *AspATs* in populus: gene expression variation and enzyme activities in response to nitrogen perturbations. Forests 10 (5), 449. https://doi.org/10.3390/f10050449.
Sun, T., Li, X.H., Liu, R.P., Mao, Z.J., Li, N., Han, Y.Y., Ding, Y.Y., Duan, X.H., 2015. Dynamic changes of atmospheric nitrogen wet deposition during growing seasons in Maoershan Area in Northeast China. Bull. Bot. Res. 35 (4), 554–558.
Sutton, M.A., Fowler, D., Burkhardt, J.K., Milford, C., 1995. Vegetation atmosphere exchange of ammonia: canopy cycling and the impacts of elevated nitrogen inputs. Water, Air, Soil Pollut. 85 (4), 2057–2063.
Takahashi, M., Higaki, A., Nohno, M., Kamada, M., Okamura, U., Matsui, K., Kitani, S., Morikawa, H., 2005. Differential assimilation of nitrogen dioxide by 70 taxa of roadside trees at an urban pollution level. Chemosphere 61, 633–639.
Takeuchi, J., Okamoto, M., Mega, R., Kanno, Y., Ohnishi, T., Seo, M., Todoroki, Y., 2016. Abscinazole-E3M, a practical inhibitor of abscisic acid 8′-hydroxylase for improving drought tolerance. Sci. Rep. 6, 37060. https://doi.org/10.1038/srep37060.
Vidmar, J.J., Zhuo, D., Siddiqi, M.Y., Schjoerring, J.K., Touraine, B., Glass, A.D.M., 2000. Regulation of high-affinity nitrate transporter genes and high-affinity nitrate influx by nitrogen pools in roots of barley. Plant Physiol. 123, 307–318.
Wang, K., Diao, J., Yang, R., Hu, Y.B., Sun, G.Y., 2015. Effects of leaf-spraying nitrate on stomatal dynamics and photosynthesis of *Syringa oblata* Lindl. leaves. Bull. Bot. Res. 35 (6), 843–847.
Wang, Y., Guo, H.Y., Hu, Y.B., Zhang, X.L., Sun, G.Y., 2017. Effects of foliar nitrogen treatment and pruning on leaf morphology and photochemical efficiency of *Populus alba* × *Populus berolinensis*. J. Southwest For. Univ. 37 (5), 48–54.
Weibull, J., Ronquist, F., Brishammar, S., 1990. Free amino acid composition of leaf exudates and phloem sap: a comparative study in oats and barley. Plant Physiol. 92, 222–226.
Wellburn, A.R., 1990. Tansley Review No. 24 Why are atmospheric oxides of nitrogen usually phytotoxic and not alternative fertilizers? New Phytol 115 (3), 395–429.
Wu, H., Fu, B., Sun, P.P., Xiao, C., Liu, J.H., 2016. A NAC transcription factor represses putrescine biosynthesis and affects drought tolerance. Plant Physiol. 172, 1532–1547.
Xu, Y., Xiao, H.Y., 2017. Free amino acid concentrations and nitrogen isotope signatures in *Pinus massoniana* (Lamb.) needles of different ages for indicating atmospheric nitrogen deposition. Environ. Pol. 221, 180–190.
Zhang, C.C., Zhou, C.Z., Burnap, R.L., Peng, L., 2018. Carbon/nitrogen metabolic balance: lessons from Cyanobacteria. Trends Plant Sci. 23 (12), 1116–1130.